CHAPTER 3

AN ECONOMIC ANALYSIS AND ECONOMETRIC INVESTIGATION OF ORDINARY CONGESTION

3.1 Introduction

The speed-flow economic analysis of the marginal external costs of congestion is, as is shown in the review Chapter, the dominant model of the economics of road congestion. However, it is argued, in the review and the present Chapter, that the analysis suffers from four problems. Firstly, the analysis considers an increase in the aggregate distance travelled by all road users in a given time period and does not explicitly consider the impact of one extra vehicle driving an additional distance in this period and reducing the distance driven by other road users. Secondly, the costs considered are those that occur during the time taken for the extra vehicle to travel this distance.[1] Thirdly, and following from the first two problems, the impact of one vehicle travelling an additional distance is to cause congestion to those on the road at the same time and their trips take longer. The journey times for these other users are longer and, in this additional time, these users in turn cause congestion to other road users. This adjustment process continues until the level of additional road use dampens to zero or a period of non-congested traffic is reached in which additional use can be accommodated with no fall in traffic speeds. Finally, the conventional model of the economics of road congestion does

[1] This approach is essentially a one period model and ignores the objective of many travellers to complete journeys by a certain time and anticipated congestion will lead them to start journeys earlier or, alternatively, those travellers who wish to start a journey at a particular time will in the face of anticipated congestion have to arrive later.

not consider the cost of increased congestion on desired journey start and finish times, i.e. the timing related congestion costs apart from the increased time to make journeys.

This Chapter develops a theory of ordinary (non-hyper) congestion on a uniform road section for the case of uniform road users with perfect knowledge of traffic conditions. It is based on the proposition that it is density of road users that causes congestion and is shown how the theory relates to the standard speed-flow analysis. The Chapter also shows how the theory can be applied to real world data taken from the measurement of speeds and flows in the Central London area. These data are used to estimate marginal external congestion time costs on different roads and shows the relative difference compared to the conventional approach. It should be pointed out that the external congestion time costs associated with less desirable start and finish journey times cannot be easily determined and are absent from the marginal external cost estimates presented here.

3.2 Theoretical Model of Ordinary Congestion

This Chapter analyses the marginal external congestion cost using speed density relationships. Traffic density D is the number of identical vehicles along a finite length of a uniform road, traffic flow F is the flow rate of vehicles that pass a given point of the road and V is the traffic speed (by definition the same for all vehicles). All variables are measured in continuous time.

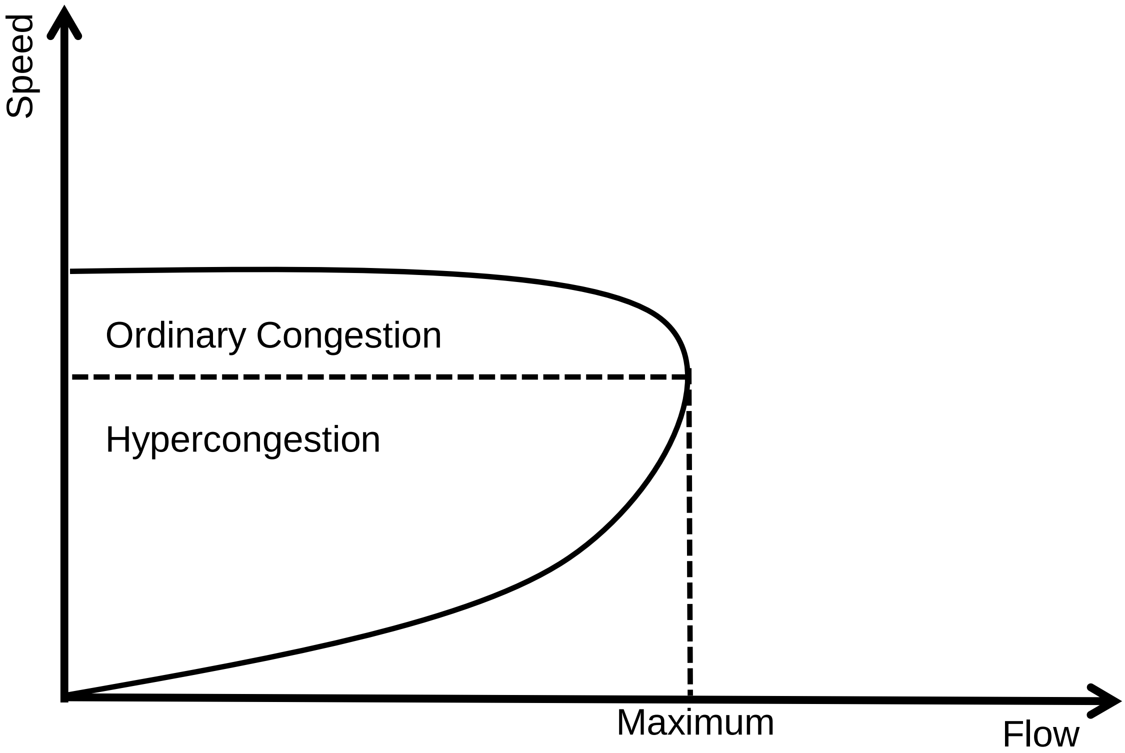

Figure 3.2.1 The Conventional Speed-Flow Relationship

An increasing traffic flow *F* decreases speed *V* as depicted in the top half of Figure 3.2.1 and discussed in the congestion literature in Chapter 2.

There is an identity between flow, density and speed:

$$F = D\,V \tag{3.2.1}$$

The calculation of the marginal external cost depends on the costs of transport. The average and total cost per vkm[2] are given by (*a* is the fixed cost of a vkm and *b* is the value of time)

$$AC = a + \frac{b}{V} \tag{3.2.2}$$

[2] vkm stands for vehicle-kilometre.

$$TC = F \ AC \tag{3.2.3}$$

The traditional presentation of the marginal external costs considers the impact of an additional vkm on speed and consequently total costs. The marginal external cost is given by the second term of

$$\frac{dTC}{dF} = AC - F \ \frac{b}{V^2}\frac{dV}{dF} \tag{3.2.4}$$

However, this traditional method requires further consideration. If there is an additional vehicle on the road in a period of ordinary congestion, then the total flow increases. This increase is a net increase as the additional vehicle travels (*V-dV)* kilometres in one time period but the all other vehicles travel less by *D dV*. It is this reduction in distance travelled by other vehicles that is the external effect and the cost is the time taken to make up these lost kilometres. This time must occur in other time periods. The cause of external congestion costs is now examined in terms of occupation or road density and this is related to the traditional method that focuses on distance travelled as the cause of congestion. In particular, it is shown how the two approaches are related.

The impact of an additional vehicle on this road for a time *dt* is depicted in Figure 3.2.2. As marginal external effects are derived through calculus, it is appropriate to consider the additional vehicle to be present for an infinitesimally small period of time *dt*. The horizontal lines represent the journey times (prior to the presence of the additional vehicle) of other vehicles. As other vehicles travel a finite distance, their journey times must also be finite and greater than the infinitesimal period *dt*. The rectangle of width *dt* represents the presence of the additional vehicle. This

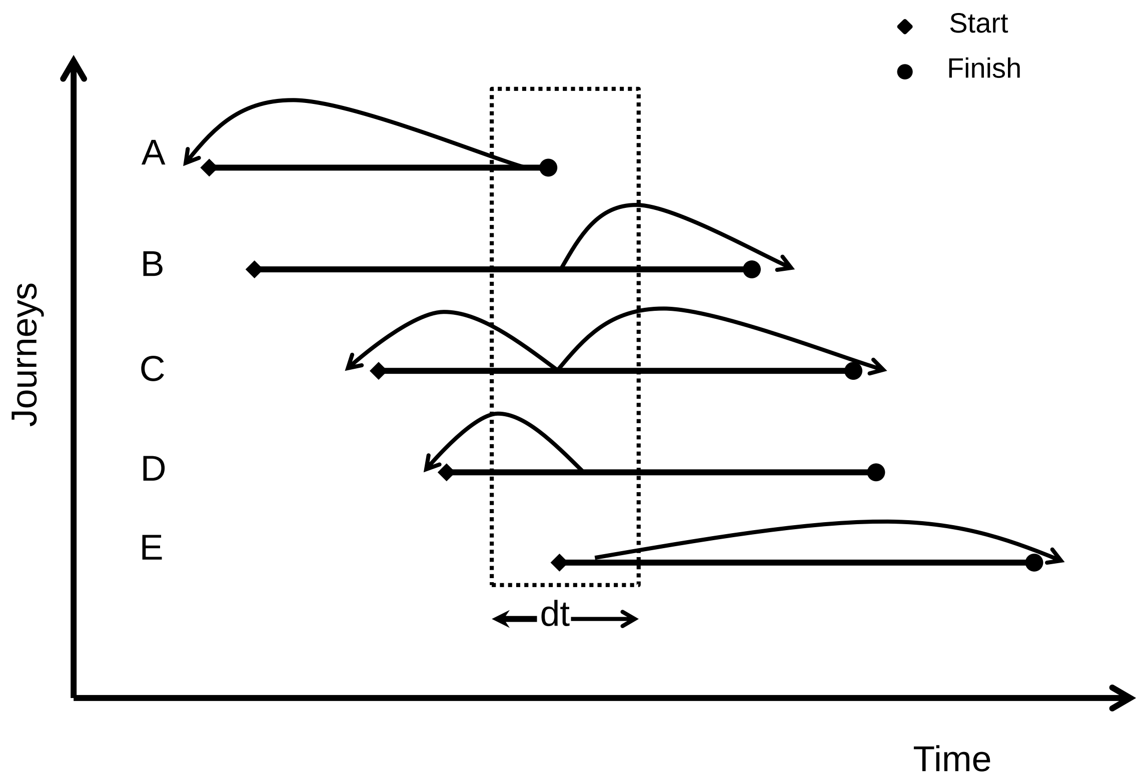

Figure 3.2.2 The Impact of an Additional Vehicle on Other Road Users

presence slows all vehicles for this period of time. Those road users who want to finish their journey by a certain time have to start earlier and those who wish to start at a particular time must finish their journey later.[3] What is important is that unless journeys start or finish in this time period, *dt,* the additional journey time must take place outside this period. So existing vehicles have to spend longer over their journey as their speeds in the period when the additional vehicle is on the road are less and the distance length of the existing vehicle journeys do not change. Thus, the impact of the additional vehicle and consequent reduction in speed is to cause congestion at other time periods. The exact calculation of this

[3] Journeys could start earlier and finish later. The results of the analysis would not be altered. In the diagram, the extra time taken for journeys is depicted by the arrows lying either to the left of the previous start time or right of the previous finish time or both.

congestion is complex as it requires information about length of journeys, speeds at end and beginning of journeys and changes in the choices of road users in starts and finishes of journeys.

The development of a new model of the external costs or congestion is based on the upper arm of Figure 3.2.1, i.e. where there is capacity for additional use of the road. In the time *dt*, the presence of another road user decreases all other road users speed by *dV*. Thus, this lost vkm in the period *dt* is

$$D\ dV\ \ dt \qquad (3.2.5)$$

It is important to note that these lost vkm are those caused by the initial additional travel of the hypothetical extra road user. They do not include the external effect caused by the additional external effect caused by the road users who have been slowed down having to complete their journeys at a later (or earlier) time. This effect is consider later in this section and is important in constructing the correct measure of marginal external congestion cost.

The lost vkm in equation (3.2.5) can be normalised by the distance travelled by the additional hypothetical road user, which is

$$dD\ V\ \ dt \qquad (3.2.6)$$

A normalized measure of a marginal external congestion effect of lost vkm is derived by division through by lost vkm expression (3.2.6) to give (as noted above, this is not the complete marginal external congestion effect)

$$\frac{dV}{dD} \quad \frac{D}{V} \qquad (3.2.7)$$

This measure has an obvious interpretation as the elasticity of speed with respect to density. In general, it is difficult to translate this measure into a time or money measure of the marginal external congestion cost for three reasons all of which are dealt with in this thesis. Firstly, knowledge is required of the traffic speeds when the lost vkm are made up so as to give completed journeys. Secondly, the external congestion generated by these lost vkm being made up have to be added in to the complete marginal external cost. Thirdly, the demand response of road users to longer journey times has to be included in the analysis.

With regard to the first issue, an over simple but useful exploratory assumption is to take these speeds as the same as when the additional road user travelled. Thus, the normalised time cost of marginal external congestion cost becomes

$$\frac{dV}{dD} \quad \frac{D}{V^2} \qquad (3.2.8)$$

This additional time costs are illustrated by the shaded areas in Figure 3.2.3 and occur either at the end or beginning of previous journey finishes or starts or both.

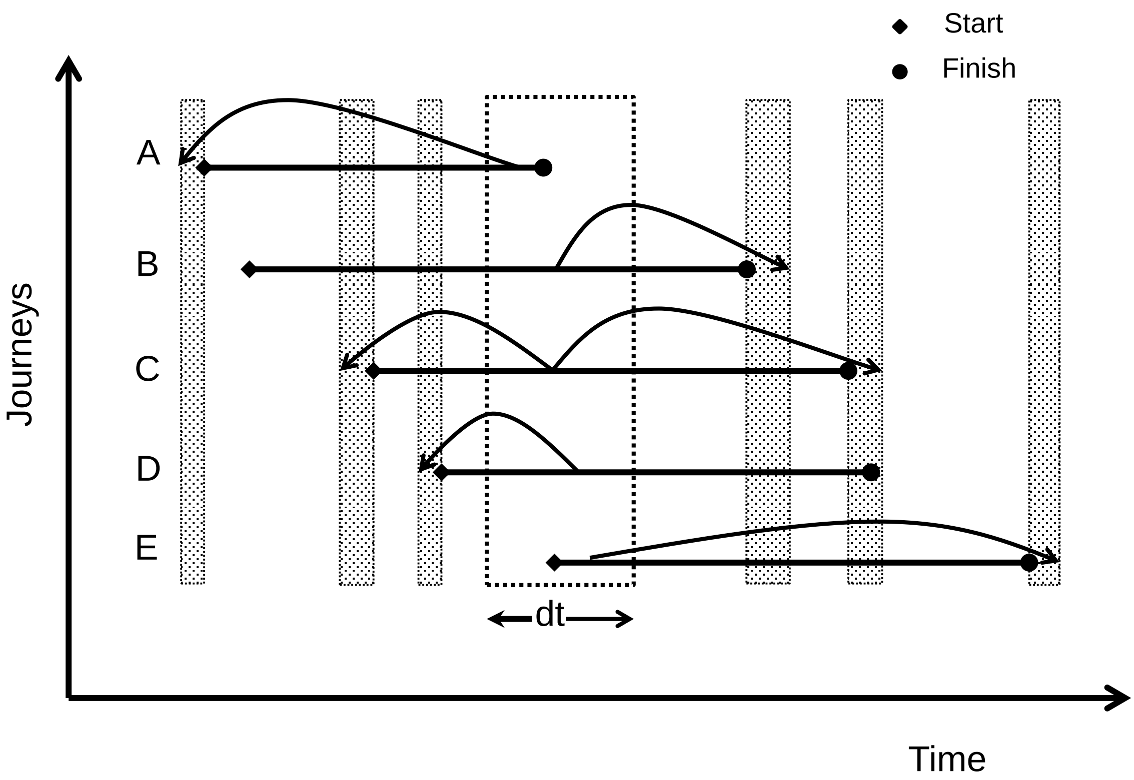

Figure 3.2.3 The Marginal External Time Cost of Additional Journey Time *dt*

The existing vehicles spend longer on the road as their speed is reduced in the period *dt* and, thus, take longer to complete their journeys.

Measuring this time cost in terms of money (see the term *b* in equation 3.2.2) gives

$$b \quad \frac{dV}{dD} \quad \frac{D}{V^2} \qquad (3.2.9)$$

There is a relation between the two external congestion cost expressions given by the second term in (3.2.4) and the full equation (3.2.9). This relation can be examined through considering a change in flow *dF* broken down into that caused by changes in density and speed

$$dF = dD\,V + dV\,D \qquad (3.2.10)$$

The expression (3.2.10) can be used to explain the differences between the two derivatives dV/dF and dV/dD

$$\frac{dV}{dF} = \frac{dV}{(dD\ V + dV\ D)} = \frac{1}{V}\ \frac{dV}{dD}\ \frac{1}{\left(1 + \varepsilon_{VD}\right)} \tag{3.2.11}$$

Thus,

$$\frac{\varepsilon_{VD}}{\left(1 + \varepsilon_{VD}\right)} = \varepsilon_{VF} \quad or \quad \varepsilon_{VD} = \frac{\varepsilon_{VF}}{1 - \varepsilon_{VF}} \tag{3.2.12}$$

Consequently, relating the analysis here to the traditional marginal external cost of congestion expression gives (it should again be noted that the left hand side of the expression below is not the full marginal external cost of congestion, see later for a full explanation of the important additions that have to be made to this latter expression)

$$\begin{aligned} b\ \frac{dV}{dD}\ \frac{D}{V^2} &= \frac{b}{V}\ \frac{dV}{dD}\ \frac{D}{V} \\ &= \frac{b}{V}\ \frac{\varepsilon_{VF}}{1 - \varepsilon_{VF}} \end{aligned} \tag{3.2.13}$$

Thus, the relative difference between the traditional expression for the marginal external congestion cost and the expression (3.2.9) is the factor $1/(1-\varepsilon_{VF})$. However, for congestion at peak times, the congestion effect represented by the left hand side will be an overestimate as the lost distance will be made up at times when speeds are greater than at the peak. Similarly, for congestion at off-peak times, this will be an underestimate as the lost distance will be made up at times when speeds are lower than at the off-peak. These types of effects are considered later in this chapter where different speeds across the day are allowed for.

It is shown later that the marginal external congestion cost can be expressed in terms of dV/dD or the corresponding elasticity. The equations (3.2.11) and (3.2.11) are of great importance as they provide a means of estimating the marginal external congestion cost even though the derivative dV/dD is not directly observable. The derivative dV/dF and the elasticity $\frac{dV}{dF}\frac{F}{V}$ are both directly observable from empirical data and can be used to estimate both dV/dD .and $\frac{dV}{dD}\frac{D}{V}$.

It has been emphasised here that the expression (3.2.9) does not capture the full congestion effect of an additional vkm as there are further congestion effects from the existing vehicles on the road completing their journeys (either earlier or later) and are not taken account of in (3.2.9). It is important to recognise that the additional journey time implied (3.2.9) in turn causes additional congestion.

This effect can be investigated but oversimplified by assuming that all journeys are infinitesimally small and that the level of density is constant across all time periods. These additional journey times lead to further congestion in an infinite regress. The impact of the first additional vehicle on reducing the distance travelled by other vehicles is given by

$$dV\ D\ dt = \varepsilon_{VD}\ V\ dD\ dt \qquad (3.2.14)$$

This distance $dV\ D\ dt$ has to be made up outside the period *dt* (unless the journey starts or finishes within this period). Thus, the additional journey time of these other vehicles has to be undertaken at a later or earlier period. With a constant density and traffic speed, it makes no difference to the additional journey time when these vehicle kilometres occur and the additional time loss is given by

$$\frac{dV\ D\ dt}{V} \;=\; \varepsilon_{VD}\ dD\ dt \qquad (3.2.15)$$

The increased density from these additional journey times lead to further congestion in an infinite regress with the relationship, at each stage of the regress, between the additional density for a period of time and the lost vehicle time caused by the increase in density been given by the elasticity of speed with respect to density. Thus, the aggregate additional journey time caused by this initial additional vehicle impact is

$$\frac{V\,dD\,dt}{V}\ \left|\varepsilon_{VD}\right|\ \left(1+\left|\varepsilon_{VD}\right|+\left|\varepsilon_{VD}\right|^2+\ldots\right) \;=\; dD\ dt\ \frac{\left|\varepsilon_{VD}\right|}{\left(1-\left|\varepsilon_{VD}\right|\right)} \qquad (3.2.16)$$

The total additional journey time caused by this initial additional vehicle impact is derived assuming constant speed and, most importantly, the elasticity $\left|\varepsilon_{VD}\right|$ is less than one. This last assumption defines ordinary congestion and the case of $\left|\varepsilon_{VD}\right|$ being greater than one, ie a situation of hypercongestion, is considered in the next chapter.

Thus, the aggregate time cost per initial additional vehicle kilometre is the ratio of the expression (3.2.10) to the additional distance travelled $(V\ dD\ dt)$

$$\frac{\left|\varepsilon_{VD}\right|}{V\left(1-\left|\varepsilon_{VD}\right|\right)} \;=\; \frac{\varepsilon_{VF}}{V} \qquad (3.2.17)$$

Multiplication by the value of time *b* gives the aggregate cost of an additional vehicle kilometre

$$\frac{b}{(1-|\varepsilon_{VD}|)}\frac{D}{V^2}\frac{dV}{dD} = \frac{b}{V}\ \varepsilon_{VF} \tag{3.2.18}$$

This expression is exactly the same as the final expression for the traditional calculation of the marginal external cost given in (3.2.4) but is not the exactly correct statement of the true marginal external congestion cost. The true external effect has also to take account of the possibility of changes in the behaviour of road users consequent on the greater costs following the initial addition time spent on the road by all users.

The long run effect of more congestion and longer journey times is to reduce the demand for transport. However, in the very short run, there is unlikely to be any major change in demand. In the longer run, the effect on demand is modelled using the derivative of demand for transport (represented by flow F) with respect to journey time, denoted by T. The effect of greater travel is to increase the time cost of travel. For an initial unit increase in vkm, there is an increase $\left.\frac{\partial T}{\partial F}\right|_{TF}$ in journey time. These changes in journey times time take place at any time before or after the initial unit increase in vkm. For a one unit increase in journey time, there is a reduction $\left.\frac{\partial F}{\partial T}\right|_{FT}$ in demand.[4] Again this reduction in demand for travel takes place at any time before or after the initial increase. Thus, an initial increase of one vkm by a particular vehicle results in a decline in demand of

---

[4] It should be noted that the derivative $\left.\partial T/\partial F\right|_{TF}$ represents the effect of congestion on journey times and $\left.\partial F/\partial T\right|_{FT}$ represents the effect of increased journey time on demand for travel.

$$\left.\frac{\partial F}{\partial T}\right|_{FT} \quad \left.\frac{\partial T}{\partial F}\right|_{TF} \tag{3.2.19}$$

The expression (3.2.13) can be used to solve for the net effect of an increase in the vkm by one user accounting for the decrease in demand by other users because of the fall in traffic speed and increase in journey times. The net increase in vkm is denoted by $(1-\gamma)$ and the effect of this net increase is to reduce demand by γ, ie

$$\gamma \;=\; \left.\frac{\partial F}{\partial T}\right|_{FT} \quad \left.\frac{\partial T}{\partial F}\right|_{TF} \; (1-\gamma)$$

$$= \left(\left.\frac{\partial F}{\partial T}\right|_{FT} \frac{D}{F}\right) \; \frac{F}{D} \quad \frac{\varepsilon_{VD}}{1+\varepsilon_{VD}} \quad \frac{1-\gamma}{V} \tag{3.2.20}$$

$$= \varepsilon_{FT} \quad \frac{\varepsilon_{VD}}{1+\varepsilon_{VD}} \; (1-\gamma)$$

$$\Rightarrow \; 1-\gamma \;=\; \frac{1}{1 + \varepsilon_{FT} \;\; \varepsilon_{VD} \,/\, (1+\varepsilon_{VD})}$$

Thus, the marginal external cost caused by an initial one vkm results in a reduction in travel demand of γ and a final time cost of

$$\frac{1}{1 + \varepsilon_{FT} \;\; \varepsilon_{VD} \,/\, (1+\varepsilon_{VD})} \; \frac{\varepsilon_{VD}}{1 + \varepsilon_{VD}} \; \frac{1}{V} \;=\; \frac{1}{1 + \varepsilon_{FT} \;\; \varepsilon_{VF}} \; \frac{\varepsilon_{VF}}{V} \tag{3.2.21}$$

The following empirical work is concerned with estimating ε_{VF} and consequently ε_{VD} through use of the equations (3.2.12).

Empirical evidence exists on the elasticity of the response of demand to changes in travel times (ε_{FT}), eg see the survey on induced demand by Goodwin (1996). These empirical results are used to produce estimates of marginal congestion costs under the assumption of a fixed speed and variable speeds across the day. The development of these estimates is discussed at the end of this chapter.

The expression (3.2.24) has an important interpretation. As the level of flow approaches the turning point in Figure 3.2.1, the elasticity ε_{VF}, ie $\varepsilon_{VD}/(1+\varepsilon_{VD})$, approaches infinity. Thus, the marginal external cost approaches the inverse of the product of the speed and demand elasticity ε_{FT}. This outcome may appear strange but is the consequence of the increased congestion effect as the elasticity ε_{FT} approaches infinity. The increased congestion effect on the marginal external cost is offset by a loss of vkm due to greater deterred demand, i.e. γ is larger.

A problem that emerged in the empirical work in this thesis is now examined and it is an issue concerning error in variables. It is frequently the case but not often commented upon that flow data is measured in discrete time with observation periods varying from six minutes to one hour (see p. 67 in Highway Research Board,1965). A simple assumption that the associated error in the measurement of flow is that it is proportional to the length of the observation period and the magnitude of the flow in this period, see Figure 2.4.3 (in Chapter 2) as an example of how a longer observation may lead to greater error. The next section's analysis shows that most of the London speed-flow data resembles pictures given in Figure 2.5.3.

This simple analysis suggests that there may be errors in the flow regressors and heteroscedastic errors in the dependent variable speed. Measurement error in the regressors leads to biased OLS estimation in the case of two variable OLS regression and, in particular, a bias down in the estimated parameter. The main solution to such problems is the use of Instrument variables estimation (IV). Moreover, this is not feasible for the investigation of speed-flow relationships as there is no available instrumental variables data collected. Thus, this problem is pointed out, unlike in many statistical investigations, but cannot be solved.

In conclusion, it should be repeated that the equations (3.2.18) and (3.2.24) are of importance as they provides means of estimating the marginal external congestion cost even though the derivative dV/dD and the elasticity $\frac{dV}{dD}\frac{D}{V}$ are not directly observable.

3.3 Empirical Investigation of Congestion in London

The empirical investigation of congestion starts from the assumption that it is density that causes congestion and that it is important to distinguish ordinary congestion from hypercongestion.[5] Before the data and econometric investigation are conducted, it is important to consider a number of issues. Firstly, it is necessary to examine the appropriate manner in which to relate traffic speeds and flows. The second issue examines the types of roads on which to base the empirical investigation. The third is how to separate the data between conditions of ordinary and hyper congested flow. The fourth is to consider simple and non-linear relationships between traffic speeds and flows.

[5] Unless otherwise important, in this Chapter we refer to ordinary congestion as congestion.

Directly linked to the assumption that density causes both speeds and flows are the past empirical investigations of speed-flow relationships. In this sense, the history of relating traffic speed to traffic flow is an example of spurious regression as both variables are caused by another variable.[6] This omission in the study of congestion is not pursued in this thesis but is raised as a problem in the study of traffic speeds and flows.

It is suggested that it is important to analyse the relationship between traffic speeds and flows on both urban and trunk/motorway roads. For ordinary congestion, we only consider examples of urban London roads but in Chapter 4, hypercongestion on both urban London roads and the Chalerm Mahanakorn Expressway in Bangkok are investigated. A variety of urban London roads are examined for which data on flows and speeds are available. It is important that the flows and consequent speeds data are collected at points that can be considered to refer to road segments where traffic conditions are representative and not unduly affected by nearby traffic lights, intersections, narrowing/widening of roads, entries, exits, etc.

The data need to be carefully separated out between what is considered to be ordinary congested and hypercongested flows. The important point is that a turning point is identified that gives the maximum flow. This can only be achieved through observation of the data and making a judgement that is tested for robustness by examination of alternative choices. Unfortunately, such procedures are in part subjective.

[6] See for details Wooldridge (2009); Gujarati (2004) and Baum (2006).

Regression models are estimated on all data sets for simple linear, quadratic, log, quadratic in logs, linear SPLINE and SPLINE in logs relationships between speeds and flows. These specifications are used to give simple estimates of elasticities and then allow estimation of potential non-linear effects. The data is also pooled to give more efficient estimation and appropriate restrictions are tested for. All estimated specifications have appropriate diagnostic tests conducted.

3.3.1 Data Description

We investigate speed-flow relationships of cars on eight street types in Central London: Blackfrairs Bridge North, Blackfrairs Bridge South, Albert Embankment North, Park Lane North, Embankment East, Embankment West, London Bridge North and London Bridge South. The eight streets were chosen on the basis of providing sufficient and appropriate data to enable the statistical investigations. The data were collected during seven working days in late September 2008 and for 24 hours each day. The selection of these days was chosen to be over a short period so as to ensure consistency of any unobservable variables. Sunrise and sunset were more or less the same on each day. Finally, there were no major or moderate changes in weather over this period (e.g. no major or moderate rain was experienced in this period) and internet searches were conducted to ensure that there were no nearby roadworks or major accidents in this period. The exact position of the flow counters on these streets is shown in Figure 3.3.1 and shows that they cover major entry points and links inside the London Central charging zone of the time[7]. Importantly, sufficient observations of speeds are available at these points to be able to undertake meaningful econometric investigation.

The traffic flows used for this study were measured by Transport for London's automatic counters for every hour. These automatic counters were located at the entry point to the charging zone in the London Congestion Charging Scheme. Our research uses 1,344 hourly flow observations (24 hours x 7 days x 8 streets). In addition, the speed observations used in this research were reported by an approximate 1,700 cars with GPRS monitoring across Greater London. The speed data were provided by TrafficLink, now called INRIX.[8] A Trafficlink car in motion with GPRS reported approximately 1.5 observations per minute or 85 observations per hour. In order to observed equilibrium speed-flow relationships, we deliberately

[7] See full detail of the London Congestion Charging Zone map at https://www.tfl.gov.uk/cdn/static/cms/documents/congestion-charge-zone-map.pdf.

[8] INRIX is a business organization providing real time traffic information. For example, INRIX supplies voice and data services for radio and television and traffic news via their commercial website service.

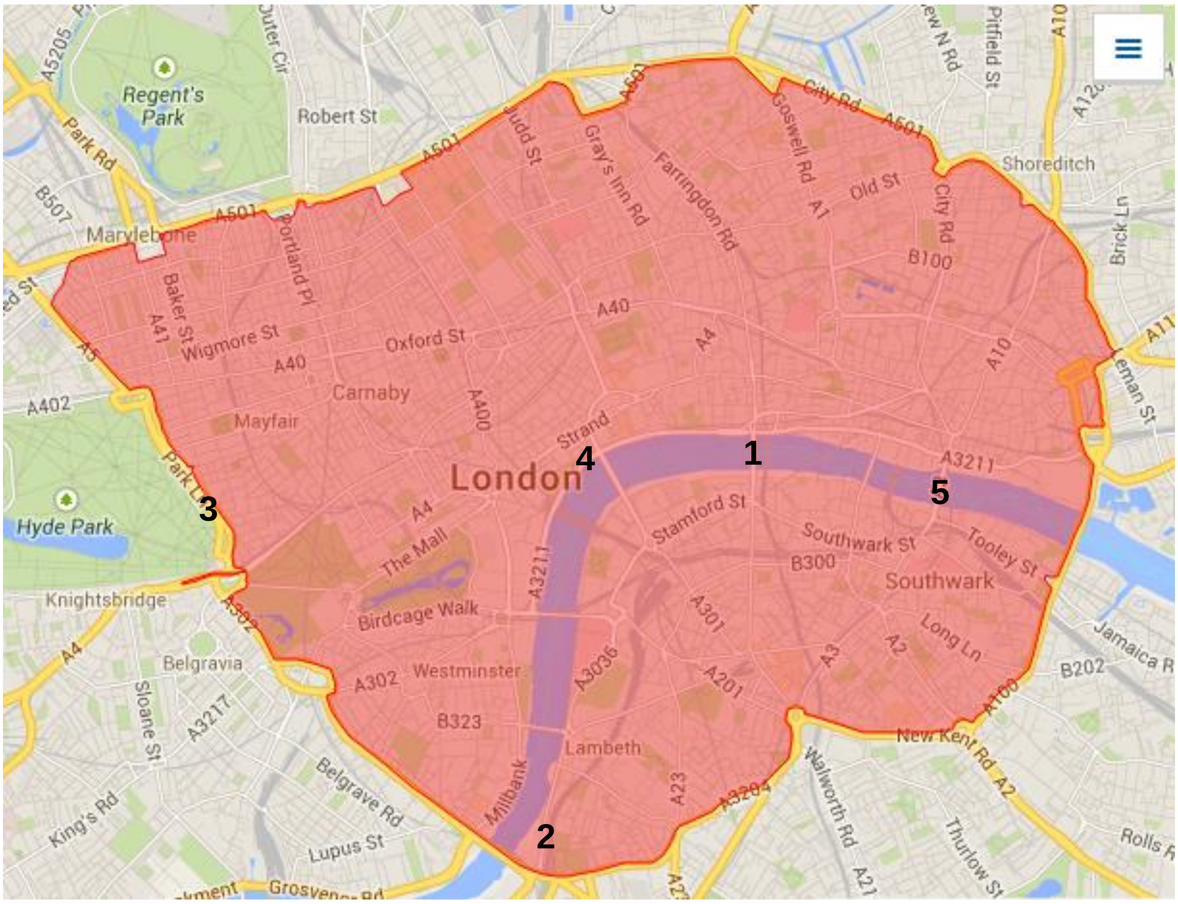

Figure 3.3.1 Locations of Eight Flow Automatic Counters (ATCs) At Entry Points and Inside The London Congestion Charging Scheme (pink shaded zone).

1: two ATCs on Blackfriars Bridge (North-South),

2: one ATC on Albert Embankment (North),

3: one ATC on Park Lane (North),

4: two ATCs on Embankment (East-West) and

5: two ATCs on London Bridge (North-South),

chose the observations on a 50 metres-length (25 metres-length before and after each automatic counter) of straight road without any immediate impediments.

The location of each automatic counter in LCCS was provided with a non-decimal figure of North/East coordinates by Transport for London. We, then, converted these figures to decimal coordinates by using an online coordinate converter.[9] We also used the Earth Point converter to locate each latitude and longitude decimal point on a map provided on Google Earth.[10] [11] The Google Earth tool allows us to measure a nearly accurate distance from each automatic counter. Moreover, it can indicate the decimal latitude and longitude of each location. This special function on Google Earth allowed us to define two rhomboid boundaries (each of 25 metres x a street width) with latitude and longitude decimal points. This allowed the relevant speed measurements to be accessed from INRIX's data set of all speed observations within the M25 boundary during this seven day period; which were labelled with longitude and latitude observations.

As discussed earlier, flows were observed at every hour, whereas speeds were observed at one moment a time. For this reason, flows were interpolated to the estimated time for the tracked cars to arrive at the counters. The orientation and structure of these roads are detailed in Appendix A3.1.

The eight speed-flow observations on these streets are shown in Figure 3.3.2. Obviously, the relationships are not in a typical parabolic shape of Figure 3.2.1 (excluding Albert Embankment North which can be seen as a typical negative

---

[9] a free software, see detail at www.nearby.org.uk/coord.cgi?f=conv.

[10] a free converter tool for Google Earth, see detail at www.earthpoint.us/convert.aspx.

[11] a free virtual globe, map and geographical information software, see detail at www. play.google.com/store/apps/details?id=com.google.earth.

slope of the top half of the parabola.). For seven of the eight relationships, there is an initial negative slope and then a broad vertical band as speed falls and flow shows considerable noise in the observations which is unrelated to speeds.[12]

With the pattern observed in Figure 3.3.1 or in the standard parabola of Figure 3.2.1, it is important to separate out the two halves of the speed-flow relation. In the case of the standard expected relationship of Figure 3.2.1, it is not possible to estimate both arms of the relationship with speed as the dependent variable, e.g. a regression of speed against flow.[13] In the case of the relationship suggested for most of the data in Figure 3.3.1, there are two very distinct parts of the relation and it is sensible to separate out the vertical part from the negative slope. The second part of these speed-flow relationships concerns hypercongestion or near hypercongestion. As Chapter 2 examines, this has confused many previous investigators and is analysed in detail in Chapter 4. Thus, the present statistical investigation focuses only on the ordinary congestion part of the speed-flow relationship.

[12] It should be noted that observations with zero speed are not reported in Figure 3.3.1 or the regresssions as they may well represent vehicles that have chosen to be stationary, e.g. parking.
[13] Such an impossible regression would potentially have two different speed observations for each flow observation.

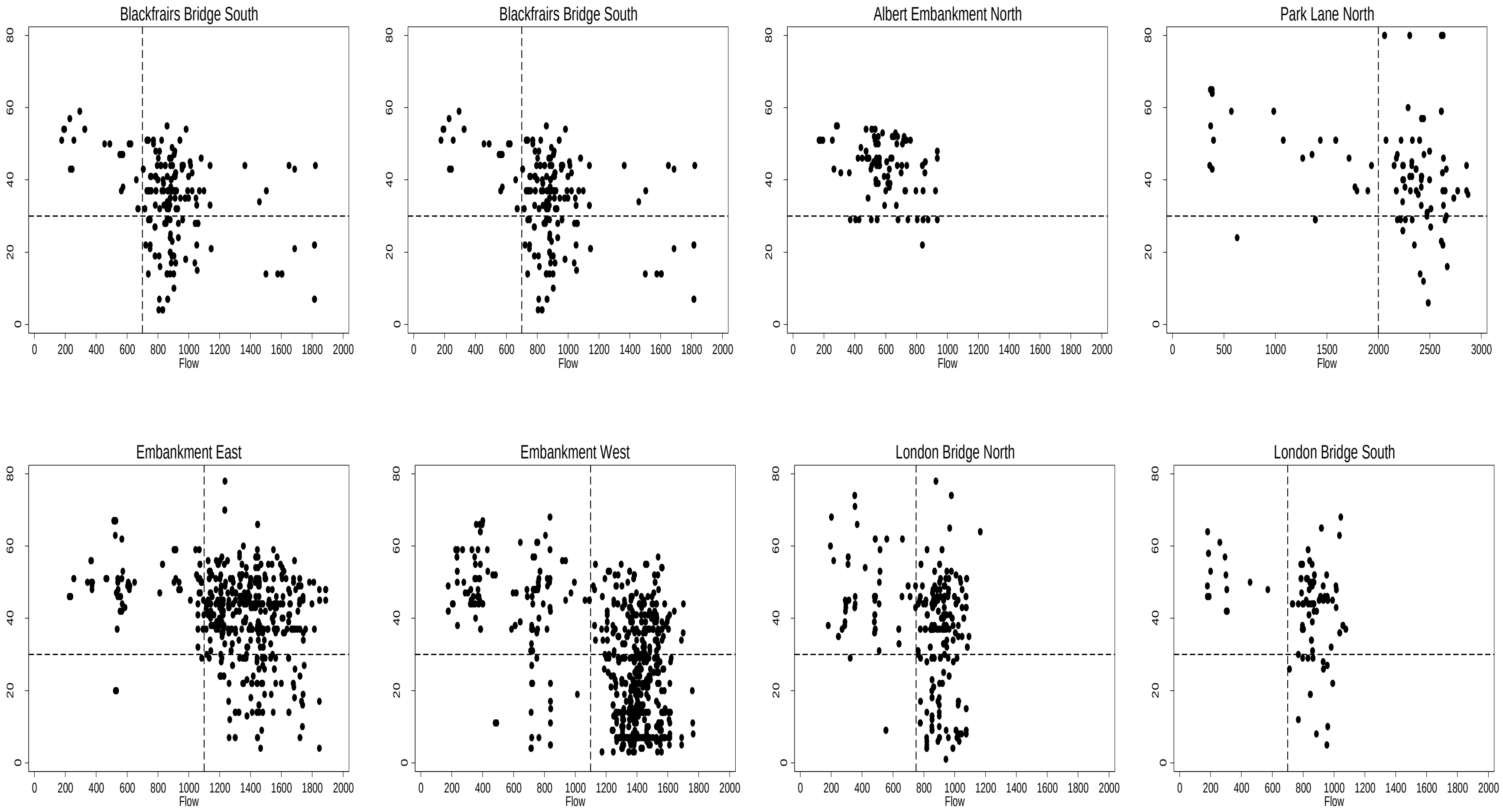

Figure 3.3.2 Speed-Flow Observations on Eight Streets in Central London (24 Hours)

How to decide whether observations represent congestion of hypercongestion is a matter of subjective judgment to an extent. We choose borderlines for each street with flow less than a certain level and speed above another level as defining ordinary congestion. These borderlines values (as shown in Figure 3.3.1) are flows of 600, 700, 2000, 1100, 1100, 750, and 700 vehicles per hour on Blackfrairs Bridge (North and South), Park Lane North, Embankment (East and West) and London Bridge (North and South), respectively. In addition, we feel sure that any speed below 30 km/h place is in hypercongested conditions and we use this borderlines to remove such observations.[14] These borderlines neatly divide up the data. Only the speed-flow pattern on Albert Embankment North is not selected with such a flow criteria.

The present Chapter examines speed-flow relationships in ordinary congestion. However, in daytime, most of the chosen roads were typically hypercongested. Thus, we only considered night time observations to ensure ordinary congestion was being considered and that the lighting was the same for all observations. Therefore, we deliberately investigated the speed-flow observations during night time hours (without day light), starting from 19.00 p.m. to 6.30 a.m. of the following day. The scatter diagrams of this speed-flow data were clearly considering ordinary congestion for six of the eight streets, see Figure 3.3.3. The shapes of speed-flow relationships on the other two streets (Blackfriars Bridge North and Embankment West) remain similar to their 24-hour observations as shown in Figure 3.3.2. In order to avoid including hypercongested observations, we applied the borderlines considered above to Figure 3.3.3 to differentiate observations between ordinary congestion and hypercongestion. After removing observations

[14] km/h stands for kilometres per hour.

on the right hand side and those under the speed 30 kilometres per hour, the more accurate speed-flow observations for ordinary congestion are given in Figure 3.3.4. We use these data sets for our further analysis.

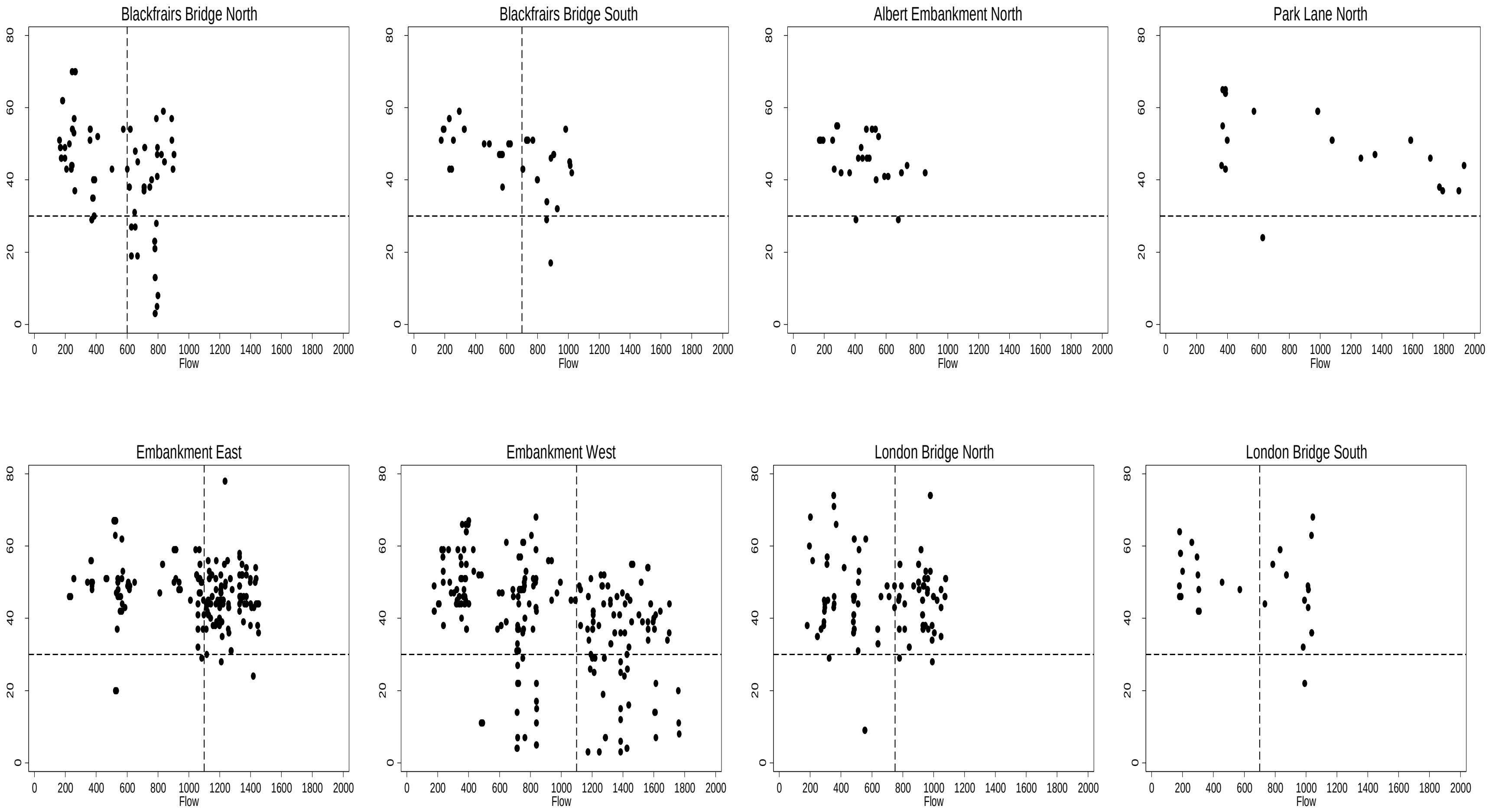

Figure 3.3.3 Speed-Flow Observations on Eight Streets in Central London (Night-Time Hours)

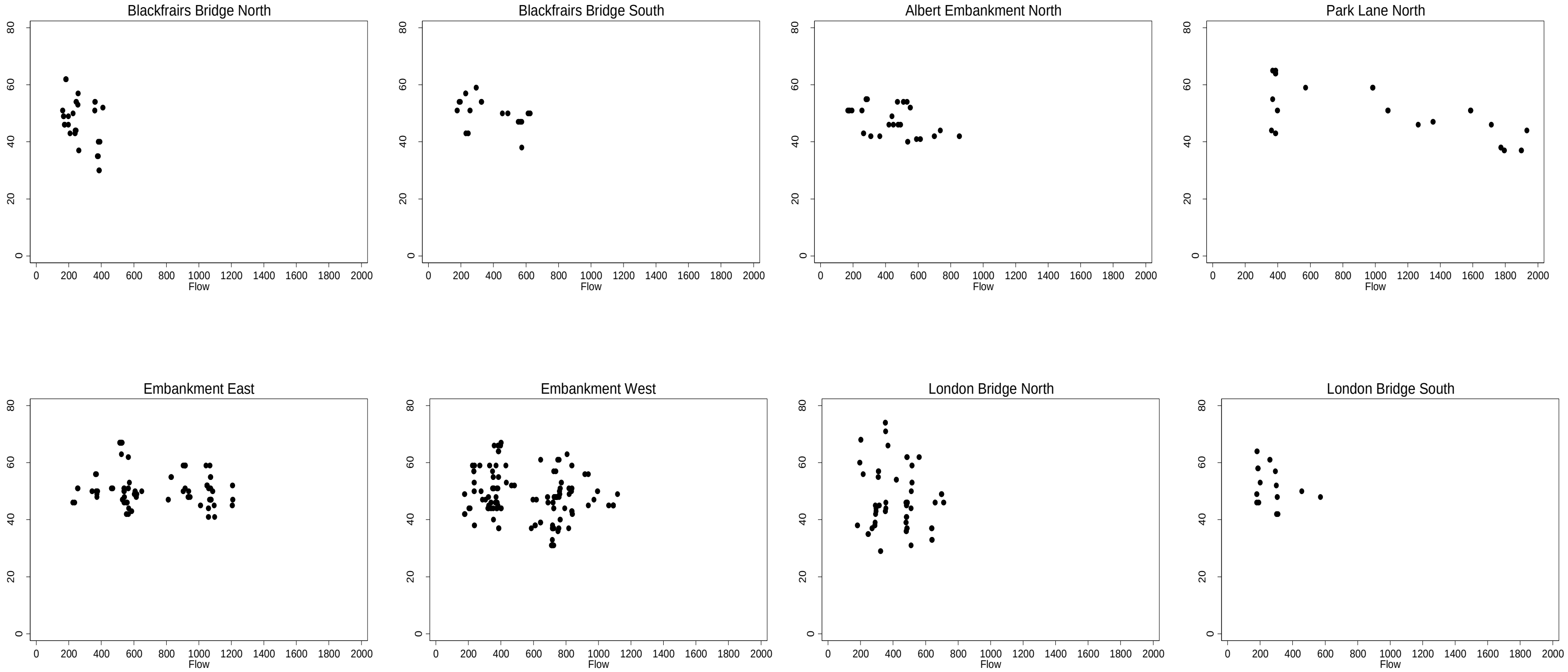

Figure 3.3.4 Speed-Flow Observations on Eight Streets in Central London (During Night-Time Hours After Removing the Likely Hypercongested Observations)

3.3.2 Analysis and Results

The statistical investigation is conducted in four parts. We first consider simple log and non-linear logarithm specifications. Then, we move on to consider linear and non-linear specifications. The economic analysis of congestion externalities presented earlier highlighted the importance of the elasticities of speed with respect to flow and density. Thus, these elasticities are estimated directly from the data for each of the eight streets using the specification

$$lnV = \alpha + \beta \, lnF + \varepsilon \qquad (3.3.1)$$

where *V* represents car speeds and *F* represents traffic flows.

The estimation of relationships of the form (3.3.1) is intended to give rough estimates of the elasticties shown to be crucial to the measurement of the external costs. It is not proposed that the resulting estimates are necessary the best statistical fit to the data.

Table 3.3.1 reports the estimation of the speed-flow relationships (3.3.1). The results in Table 3.3.1 show that all the elasticity coefficients are negative as expected. The elasticities of speed with respect to flow vary between -0.065 and -0.300. Three quarters of the estimated elasticities are statistically significantly different from zero. Two or perhaps three regressions fail the Ramsey RESET and a few fail the Jacque-Berra Normality test.[15] In addition, we draw predicted speeds corresponding to the results in Table 3.3.1 in Figure 3.3.5.

Next, we adjust the specification by aggregating all observations of eight streets into a single data set. In order to check whether we can use the same log model

[15] The regressions that failed White and Chi-squared heteroscedascity test are already adjusted with White Consistent standard errors.

for eight streets; we add intercept and slope dummy variables. In addition to the diagnostic tests, we test equality in each of the intercept and slope terms. The results show that we cannot reject the two hypotheses of equality in each of intercept and slope terms in Table 3.3.2, and a restriction of equality in intercept terms, respectively. Therefore, the final regression of aggregated data set is conducted and shown in Table 3.3.4. Additionally, eight predicted speeds corresponding to this regression are shown in Figure 3.3.6. The simple logarithm regression yields not surprisingly a statistically significant negative slope of -0.04 for each street.

Table 3.3.1 Log Speed-Flow Specifications: Dependent Variable *lnV*

Variables	BFBN	BFBS	AMBN	PKLN	EMBE	EMBW	LDBN	LDBS
Constant	5.514***	4.531***	4.481***	5.089***	4.391***	4.346***	4.380***	4.569***
	(9.65)	(14.13)	(25.11)	(16.21)	(19.86)	(24.28)	(9.04)	(12.91)
lnF	-0.300***	-0.104*	-0.102***	-0.174***	-0.065**	-0.078***	-0.089	-0.110
	(-2.84)	(-1.91)	(-3.36)	(-3.78)	(-1.97)	(-2.74)	(-1.11)	(-1.76)
Diagnostic Statistics								
Observations	32	20	27	23	97	142	60	15
F-Statistics	9.71	3.64	5.68	14.27	3.53	7.52	1.24	3.11
Adjusted R^2	0.219	0.122	0.153	0.376	0.025	0.044	0.004	0.130
Heteroscedasticity :Chi-Squared	3.81	0.11	0.48	1.08	5.22	0.00	1.29	2.28
	(0.051)	(0.741)	(0.488)	(0.298)	(0.022)	(0.958)	(0.256)	(0.131)
White Test:Chi-Squared	9.544	0.642	6.499	2.23	16.09	3.191	2.415	4.542
	(0.008)	(0.725)	(0.039)	(0.328)	(0.000)	(0.202)	(0.298)	(0.103)
RESET:F-Statistics	0.39	1.40	0.37	2.40	3.94	2.67	1.50	0.41
	(0.760)	(0.281)	(0.774)	(0.101)	(0.011)	(0.050)	(0.225)	(0.749)
Normality:Chi-Squared	4.38	7.45	3.62	2.68	4.50	0.65	5.55	0.40
	(0.111)	(0.024)	(0.164)	(0.262)	(0.105)	(0.722)	(0.062)	(0.818)

Notes:
1. BFBN, BFBS, ABEN, PKLN, EMBE, EMBW, LDBN, and LDBS denote Blackfrairs Bridge North, Blackfrairs Bridge South, Albert Embankment North, Park Lane North, Embankment East, Embankment West, London Bridge North and London Bridge South, respectively.
2. ***p<0.01; **p<0.05, and *p<0.10.
3. Any results which failed the White Test, are already adjusted with Heteroscedasticity-Consistency Standard Errors.
4. Figures in parentheses under the coefficients are ‘t-statistics’ and under the diagnostic tests are ‘p-values’.

Table 3.3.2 Log Speed-Flow Specification: Dependent Variable *lnV*

Variables	Coefficients
BFBN	5.514***
	(11.11)
BFBS	4.530***
	(9.35)
AMBN	4.481***
	(10.91)
PKLN	5.089***
	(14.80)
EMBE	4.391***
	(16.93)
EMBW	4.346***
	(24.21)
LDBN	4.380***
	(12.56)
LDBS	4.569***
	(8.58)
BFBN_lnF	-0.300***
	(-2.88)
BFBS_lnF	-0.104***
	(-2.18)
AMBN_lnF	-0.102***
	(-3.43)
PKLN_lnF	-0.174***
	(3.60)
EMBE_lnF	-0.065**
	(-1.96)
EMBW_lnF	-0.078***
	(-3.01)
LDBN_lnF	-0.089
	(-1.09)
LDBS_lnF	-0.110**
	(-2.28)

Diagnostic Statistics	
Observations	416
F-Statistics	15261.66
Adjusted R^2	0.998
Heteroscedasticity :Chi-Squared	5.25
	(0.022)
White Test:Chi-Squared	7.650
	(0.021)
RESET:F-Statistics	4.55
	(0.021)
Normality:Chi-Squared	1.56
	(0.457)
Testing Restrictions:	
(1) $H_0 : \alpha_1 = \alpha_2 = \alpha_3 = \alpha_4 = \alpha_5 = \alpha_6 = \alpha_7 = \alpha_8$	1.16
	(0.325)
(2) $H_0 : \beta_1 = \beta_2 = \beta_3 = \beta_4 = \beta_5 = \beta_6 = \beta_7 = \beta_8$	1.22
	(0.288)

Notes:

1. BFBN, BFBS, ABEN, PKLN, EMBE, EMBW, LDBN, and LDBS denote Blackfrairs Bridge North, Blackfrairs Bridge South, Albert Embankment North, Park Lane North, Embankment East, Embankment West, London Bridge North and London Bridge South, respectively.
2. ***p<0.01; **p<0.05, and *p<0.10.
3. Any results which failed the White Test, are already adjusted with Heteroscedasticity-Consistency Standard Errors.
4. Figures in parentheses under the coefficients are ‘t-statistics’ and under the diagnostic tests are ‘p-values’.

Table 3.3.3 Log Speed-Flow Specification: Dependent Variable *lnV*

Variables	Coefficients
BFBN	4.414***
	(42.89)
BFBS	4.512***
	(40.98)
AMBN	4.473***
	(40.27)
PKLN	4.595***
	(36.61)
EMBE	4.626***
	(39.38)
EMBW	4.493***
	(39.80)
LDBN	4.449***
	(40.82)
LDBS	4.516***
	(41.67)
lnF	-0.101***
	(-5.68)

Diagnostic Statistics	
Observations	416
F-Statistics	27027.43
Adjusted R^2	0.998
Heteroscedasticity :Chi-Squared	3.03
	(0.081)
White Test:Chi-Squared	5.092
	(0.078)
RESET:F-Statistics	2.63
	(0.049)
Normality:Chi-Squared	1.24
	(0.539)
Testing Restrictions:	
(1) H_0: $\alpha_1=\alpha_2=\alpha_3=\alpha_4=\alpha_5=\alpha_6=\alpha_7=\alpha_8$	1.24
	(0.539)

Notes:

1. BFBN, BFBS, ABEN, PKLN, EMBE, EMBW, LDBN, and LDBS denote Blackfrairs Bridge North, Blackfrairs Bridge South, Albert Embankment North, Park Lane North, Embankment East, Embankment West, London Bridge North and London Bridge South, respectively.
2. ***p<0.01; **p<0.05, and *p<0.10.
3. Any results which failed the White Test, are already adjusted with Heteroscedasticity-Consistency Standard Errors.
4. Figures in parentheses under the coefficients are ‘t-statistics’ and under the diagnostic tests are ‘p-values’.

Table 3.3.4 Log Speed-Flow Specification: Dependent Variable *lnV*

Variables	Coefficients
Constant	4.149***
	(43.58)
lnF	-0.042***
	(-2.74)
Diagnostic Statistics	
Observations	416
F-Statistics	7.53
Adjusted R^2	0.015
Heteroscedasticity :Chi-Squared	0.75
	(0.387)
White Test:Chi-Squared	13.781
	(0.001)
RESET:F-Statistics	0.69
	(0.558)
Normality:Chi-Squared	1.94
	(0.378)

Notes:

1. BFBN, BFBS, ABEN, PKLN, EMBE, EMBW, LDBN, and LDBS denote Blackfrairs Bridge North, Blackfrairs Bridge South, Albert Embankment North, Park Lane North, Embankment East, Embankment West, London Bridge North and London Bridge South, respectively.
2. ***p<0.01; **p<0.05, and *p<0.10.
3. Any results which failed the White Test, are already adjusted with Heteroscedasticity-Consistency Standard Errors.
4. Figures in parentheses under the coefficients are ‘t-statistics’ and under the diagnostic tests are ‘p-values’.

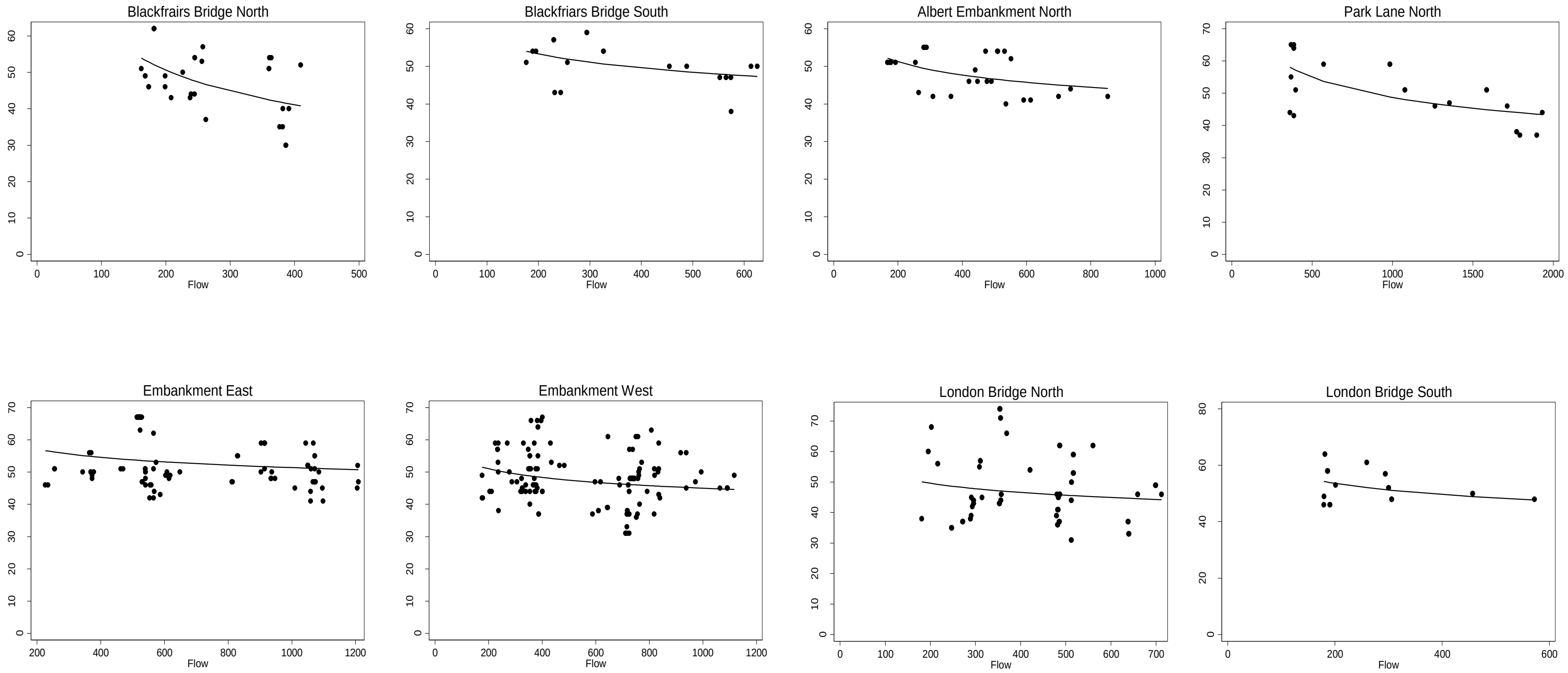

Figure 3.3.5 Speed-Flow Observations with Predicted Speeds Corresponding to Table 3.3.1 [lnV vs lnF: using street data]

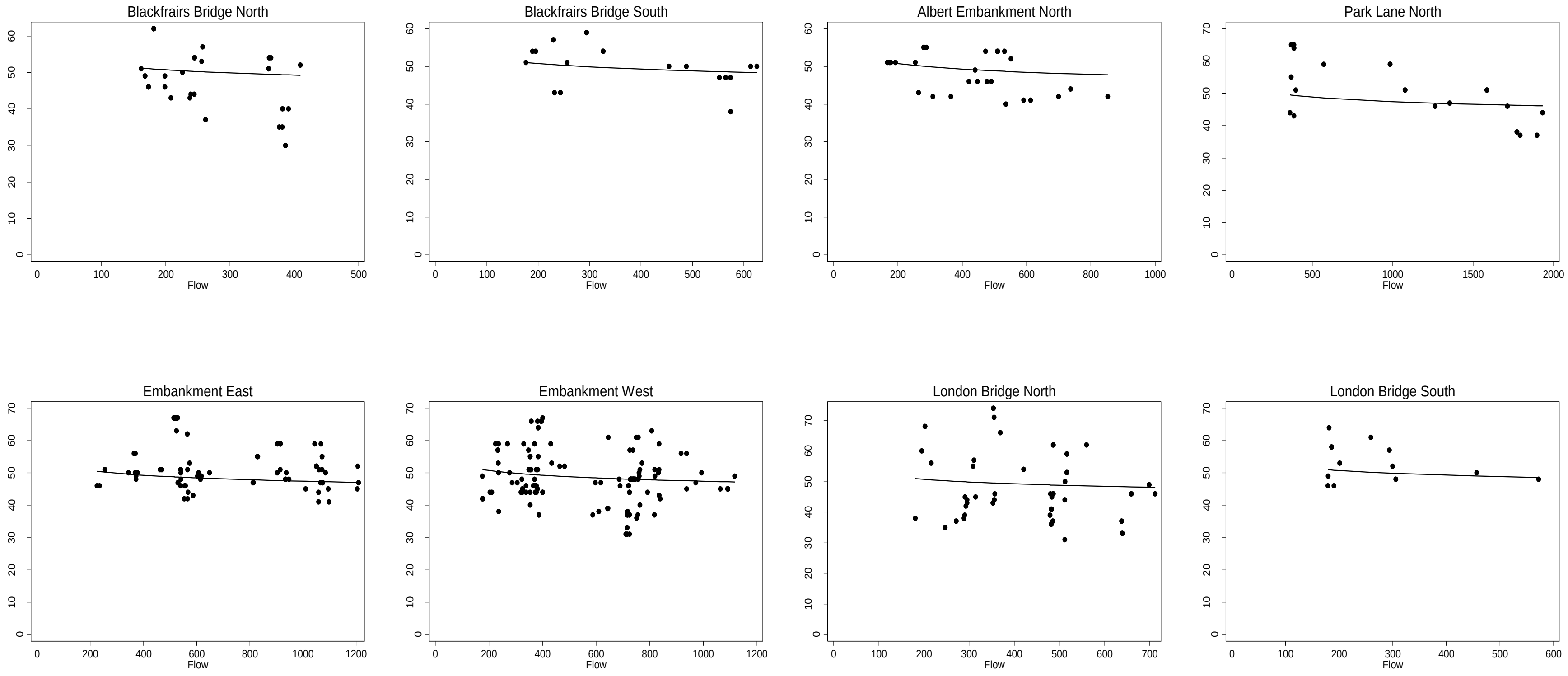

Figure 3.3.6 Speed-Flow Observations with Predicted Speeds Corresponding to Table 3.3.4 [lnV vs lnF : using street data aggregation]

It is of note that the RESET tests reported in Table 3.3.1 are mostly passed. However, the non-linearity suggested by the theory demands a more sophisticated specification is estimated. Therefore, further statistical investigation is conducted with the specification (3.3.2).

$$lnV = \eta + \gamma \; lnF + \pi \; \left(lnF\right)^2 + \mu \tag{3.3.2}$$

where *V* represents car speeds and *F* represents traffic flows.

The corresponding results and diagnostic statistics are presented in Table 3.3.5. The results suggest that only a quarter of the estimated coefficients are statistically significantly different from zero with 90% significance level and only about half of the regressions pass all the diagnostic tests. This suggests possible misspecification problems. The predicted speeds corresponding to these regressions are shown in Figure 3.3.7.

Next, we adjust the specification by aggregating all observations of eight streets into a single data set. In order to check whether we can use the same quadratic in logs specification for eight streets; we add intercept, slope and curvature dummy variables. In addition to the diagnostic tests, we test equality in each intercept, slope and curvature terms. The results in Table 3.3.6 show that we cannot reject three hypotheses of equality in intercept, slope and curvature terms. Thus, we accept the restriction on the final regression of equality of the curvature in the aggregated data set and the estimation is conducted and shown in Table 3.3.7; for which both restriction tests of equality in intercept and slope terms are rejected. Additionally, eight predicted speeds corresponding to this regression are shown in Figure 3.3.8. The quadratic logarithmic regressions mostly give statistically significant negative slopes for each street.

Table 3.3.5 Quadratic in Logs Speed-Flow Specifications: Dependent Variable *lnV*

Variables	BFBN	BFBS	AMBN	PKLN	EMBE	EMBW	LDBN	LDBS
Constant	-2.440	-2.833	1.429	-9.182*	-5.437***	3.374	0.942	0.326
	(-0.21)	(-0.46)	(0.43)	(-1.79)	(-2.60)	(1.59)	(0.12)	(0.06)
lnF	2.568	2.427	0.941	4.137***	3.011***	0.239	1.073	1.360
	(0.60)	(1.14)	(0.83)	(2.68)	(4.47)	(0.35)	(0.42)	(-0.76)
$(lnF)^2$	-0.257	-0.216	-0.088	-0.322***	-0.239***	-0.025	-0.098	-0.126
	(-0.66)	(-1.19)	(-0.92)	(-2.79)	(-4.46)	(-0.47)	(-0.45)	(-0.83)
Diagnostic Statistics								
Observations	32	20	27	23	97	142	60	15
F-Statistics	4.92	2.57	3.25	13.34	0.0006	3.82	0.71	1.86
Adjusted R^2	0.202	0.232	0.148	0.529	0.127	0.024	-0.009	0.109
Heteroscedasticity :Chi-Squared	4.12	0.16	0.03	0.56	13.72	0.02	1.30	1.72
	(0.042)	(0.688)	(0.869)	(0.453)	$(2\text{x}10^{-4})$	(0.879)	(0.255)	(0.189)
White Test:Chi-Squared	9.218	1.733	3.840	0.910	32.771	6.296	2.593	4.058
	(0.010)	(0.420)	(0.146)	(0.634)	$(7.7\text{x}10^{-8})$	(0.042)	(0.273)	(0.131)
RESET:F-Statistics	5.97	0.98	0.57	0.06	2.03	4.12	3.09	0.36
	(0.003)	(0.429)	(0.641)	(0.982)	(0.115)	(0.008)	(0.034)	(0.784)
Normality:Chi-Squared	4.07	6.68	1.75	1.11	13.11	0.84	6.79	0.51
	(0.130)	(0.035)	(0.417)	(0.574)	(0.001)	(0.655)	(0.033)	(0.775)

Notes:

1. BFBN, BFBS, ABEN, PKLN, EMBE, EMBW, LDBN, and LDBS denote Blackfrairs Bridge North, Blackfrairs Bridge South, Albert Embankment North, Park Lane North, Embankment East, Embankment West, London Bridge North and London Bridge South, respectively.
2. ***p<0.01; **p<0.05, and *p<0.10.
3. Any results which failed the White Test, are already adjusted with Heteroscedasticity-Consistency Standard Errors.
4. Figures in parentheses under the coefficients are ‘t-statistics’ and under the diagnostic tests are ‘p-values’.

Table 3.3.6 Quadratic in Logs Speed-Flow Specification: Dependent Variable *lnV*

Variables	Coefficients
BFBN	-2.440
	(-0.20)
BFBS	-2.833
	(-0.30)
AMBN	1.429
	(0.28)
PKLN	-9.182
	(-1.44)
EMBE	-5.437
	(-1.60)
EMBW	3.374
	(1.41)
LDBN	0.942
	(0.17)
LDBS	0.326
	(0.04)
BFBN_lnF	2.568
	(0.57)
BFBS_lnF	2.427
	(0.75)
AMBN_lnF	0.941
	(0.53)
PKLN_lnF	4.137**
	(2.15)
EMBE_lnF	3.011***
	(2.83)
EMBW_lnF	0.239
	(0.31)
LDBN_lnF	1.073
	(0.59)
LDBS_lnF	1.360
	(0.52)
BFBN(lnF)²	-0.257
	(-0.64)
BFBS(lnF)²	-0.216
	(-0.79)
AMBN(lnF)²	-0.088
	(-0.59)
PKLN(lnF)²	-0.322**
	(-2.24)
EMBE(lnF)²	-0.239***
	(-2.90)
EMBW(lnF)²	-0.025
	(-0.41)
LDBN(lnF)²	-0.098
	(-0.64)
LDBS(lnF)²	-0.126
	(-0.56)

Diagnostic Statistics	
Observations	416
F-Statistics	10369.82
Adjusted R^2	0.998
Heteroscedasticity :Chi-Squared	3.91
	(0.047)
White Test:Chi-Squared	4.444
	(0.108)
RESET:F-Statistics	0.03
	(0.991)
Normality:Chi-Squared	0.64
	(0.726)
Testing Restrictions:	
(1) H_0: $\eta_1=\eta_2=\eta_3=\eta_4=\eta_5=\eta_6=\eta_7=\eta_8$	0.98
	(0.442)
(2) H_0: $\gamma_1=\gamma_2=\gamma_3=\gamma_4=\gamma_5=\gamma_6=\gamma_7=\gamma_8$	0.98
	(0.445)
(3) H_0: $\pi_1=\pi_2=\pi_3=\pi_4=\pi_5=\pi_6=\pi_7=\pi_8$	0.95
	(0.468)

Notes:

1. BFBN, BFBS, ABEN, PKLN, EMBE, EMBW, LDBN, and LDBS denote Blackfrairs Bridge North, Blackfrairs Bridge South, Albert Embankment North, Park Lane North, Embankment East, Embankment West, London Bridge North and London Bridge South, respectively.
2. ***p<0.01; **p<0.05, and *p<0.10.
3. Figures in parentheses under the coefficients are 't-statistics' and under the diagnostic tests are 'p-values'.

Table 3.3.7 Quadratic in Logs Speed-Flow Specification: Dependent Variable *lnV*

Variables	Coefficients
BFBN	1.623
	(1.38)
BFBS	-1.382**
	(-2.16)
AMBN	-1.47***
	(-2.46)
PKLN	-2.114***
	(-2.59)
EMBE	-2.399***
	(-3.54)
EMBW	-2.042***
	(-3.20)
LDBN	-1.663**
	(-2.10)
LDBS	-1.274**
	(-2.01)
BFBN_lnF	1.102***
	(2.82)
BFBS_lnF	1.370***
	(3.41)
AMBN_lnF	1.379***
	(3.42)
PKLN_lnF	1.511***
	(3.26)
EMBE_lnF	1.552***
	(3.56)
EMBW_lnF	1.476***
	(3.49)
LDBN_lnF	1.405***
	(3.29)
LDBS_lnF	1.352***
	(3.35)
$(lnF)^2$	-0.126***
	(-3.68)

Diagnostic Statistics	
Observations	416
F-Statistics	6.90
Adjusted R^2	0.184
Heteroscedasticity :Chi-Squared	65.32
	(0.00)
White Test:Chi-Squared	4.815
	(0.09)
RESET:F-Statistics	1.40
	(0.241)
Normality:Chi-Squared	1.31
	(0.518)
Testing Restrictions:	
(1) $H_0: \eta_1 = \eta_2 = \eta_3 = \eta_4 = \eta_5 = \eta_6 = \eta_7 = \eta_8$	2.00
	(0.053)
(2) $H_0: \gamma_1 = \gamma_2 = \gamma_3 = \gamma_4 = \gamma_5 = \gamma_6 = \gamma_7 = \gamma_8$	2.22
	(0.032)

Notes:

1. BFBN, BFBS, ABEN, PKLN, EMBE, EMBW, LDBN, and LDBS denotes Blackfrairs Bridge North, Blackfrairs Bridge South, Albert Embankment North, Park Lane North, Embankment East, Embankment West, London Bridge North and London Bridge South, respectively.
2. ***p<0.01; **p<0.05, and *p<0.10.
3. Any results which failed the White Test, are already adjusted with Heteroscedasticity-Consistency Standard Errors.
4. Figures in parentheses under the coefficients are ‘t-statistics’ and under the diagnostic tests are ‘p-values’.

.

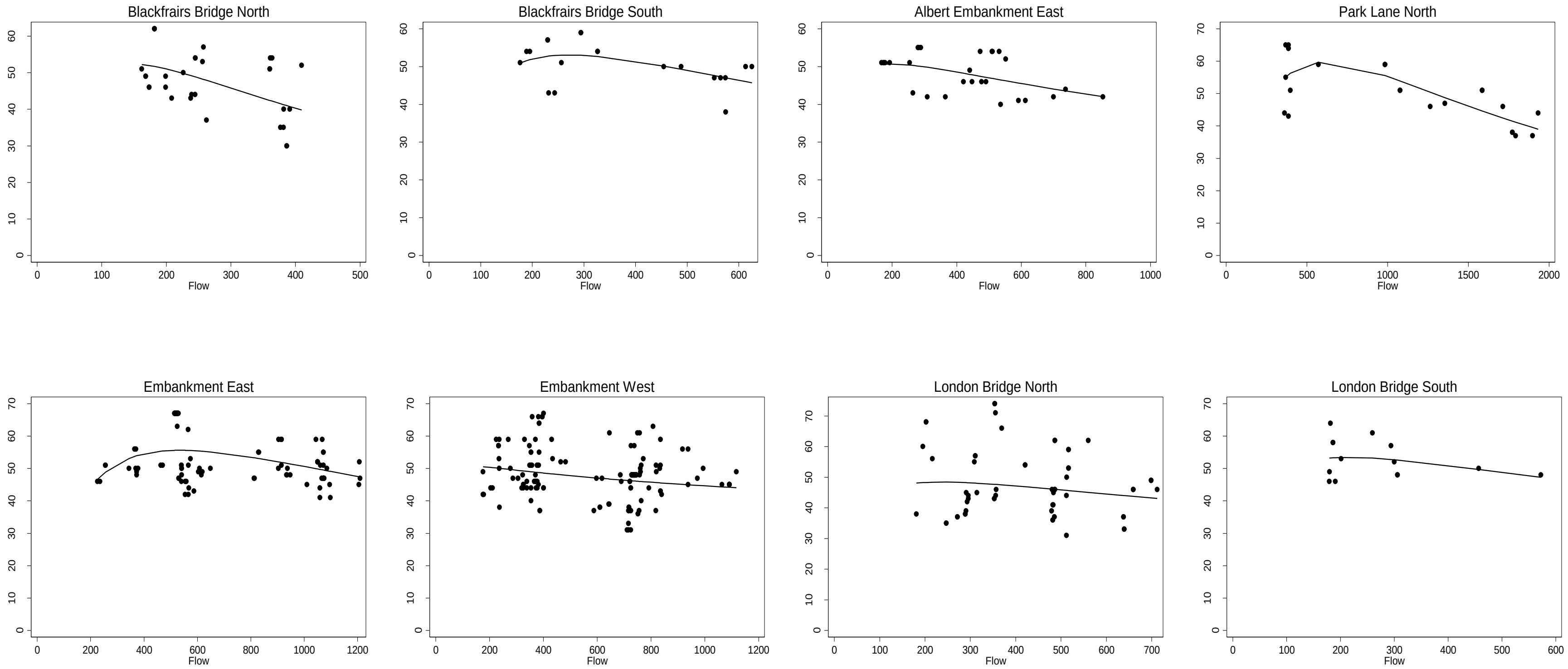

Figure 3.3.7 Speed-Flow Observations with Predicted Speeds Corresponding to Table 3.3.5 [lnV vs lnF $(\ln F)^2$:using street data]

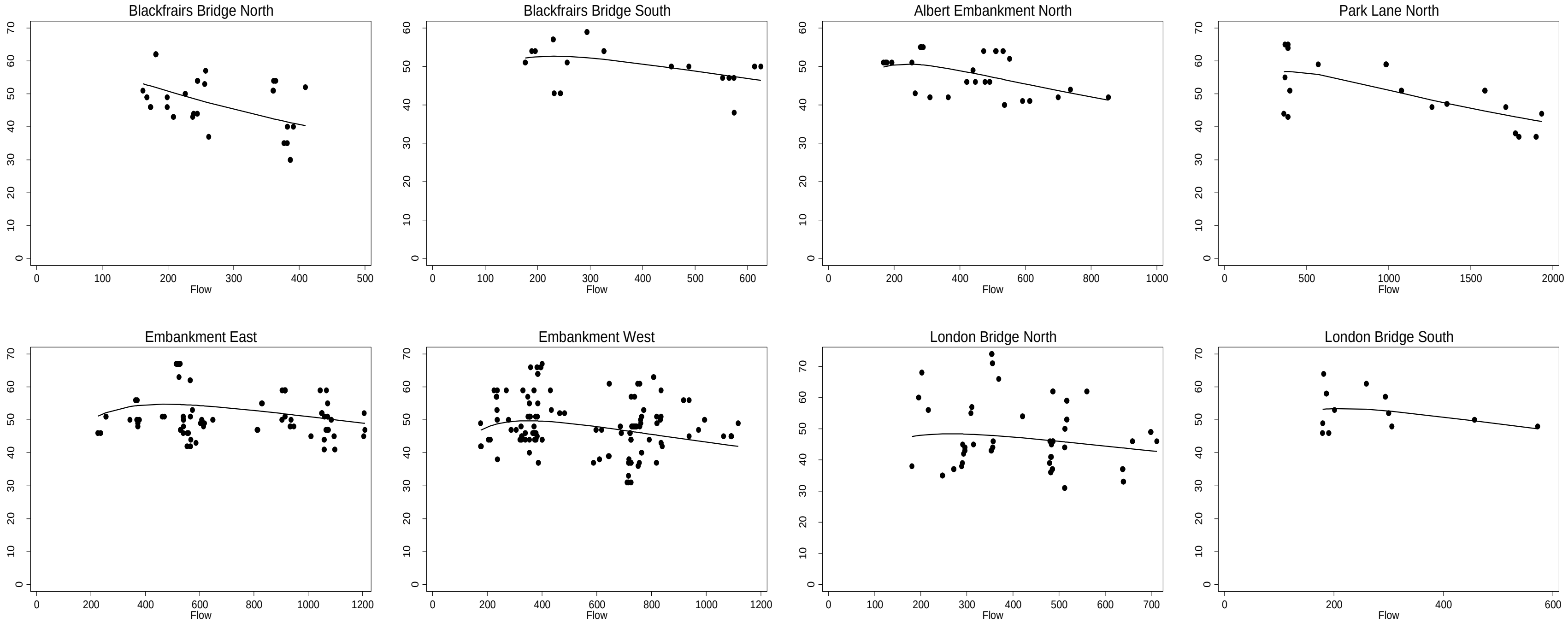

Figure 3.3.8 Speed-Flow Observations with Predicted Speeds Corresponding to Table 3.3.7 [lnV vs lnF $(\ln F)^2$:using street data aggregation]

In addition to the non-linear empirical investigation of ordinary congestion in Central London discussed above, we carry out further regressions on different specifications. However, the results though similar are on the whole slightly less statistically significant and less easy to interpret in terms of elasticities.

Firstly, we estimate the relations of car speed to flows with a simple linear model

$$V = \phi + \varphi F + \varsigma \qquad (3.3.3)$$

where *V* represents car speeds and *F* represents traffic flows.

The results and diagnostic statistics are displayed in Table 3.3.8. The results show that all but one have slope coefficients statistically significantly different from zero with 90% confidence level and all of them are negative. In considering the diagnostic tests, most regressions passed the White and Heteroscedascity tests and, for those that did not, adjusted standard errors are reported. Four of the regressions fail with the RESET or Normality tests or both. The predicted speeds of each of the regressions are shown in Figure 3.3.9.

Next, we adjust the specification by aggregating all observations of eight streets into a single data set. In order to check whether we can use the same simple linear model for eight streets; we add intercept and slope dummy variables. In addition to the diagnostic tests, we test equality of each intercept and slope terms. The results in Table 3.3.9 show that we can only accept the hypothesis of equality in slope terms. Therefore, the final regression of aggregated data set is shown in Table 3.3.10; which rejects a restriction test of equality in each of the intercept terms. Additionally, eight predicted speeds corresponding to this regression are shown in Figure 3.3.10. Unsurprisingly, the linear regressions give statistically significant negative slope for each street.

Table 3.3.8 Linear Speed-Flow Specifications: Dependent Variable *V*

Variables	BFBN	BFBS	AMBN	PKLN	EMBE	EMBW	LDBN	LDBS
Constant	61.143***	56.501***	53.709***	62.002***	58.716***	52.123***	53.354***	57.281***
	(13.42)	(19.53)	(22.36)	(21.32)	(26.66)	(31.51)	(11.97)	(18.42)
F	-0.049***	-0.015**	-0.013**	-0.010***	-0.007***	-0.007***	-0.013	-0.017*
	(-3.04)	(-2.16)	(-2.54)	(-4.47)	(-2.63)	(-2.75)	(-1.32)	(-1.87)
Diagnostic Statistics								
Observations	32	20	27	23	97	142	60	15
F-Statistics	9.21	4.67	6.44	19.98	6.90	7.59	1.74	3.50
Adjusted R^2	0.209	0.161	0.173	0.463	0.057	0.044	0.012	0.151
Heteroscedasticity :Chi-Squared	1.17	0.53	0.01	3.79	9.75	1.22	2.82	2.37
	(0.279)	(0.467)	(0.921)	(0.051)	(0.001)	(0.269)	(0.093)	(0.123)
White Test:Chi-Squared	4.47	0.56	6.11	5.67	24.09	6.04	4.09	4.92
	(0.106)	(0.755)	(0.047)	(0.058)	(0.000)	(0.048)	(0.128)	(0.085)
RESET:F-Statistics	0.08	1.69	0.29	0.85	3.42	4.21	1.66	0.13
	(0.969)	(0.212)	(0.832)	(0.484)	(0.020)	(0.007)	(0.187)	(0.942)
Normality:Chi-Squared	10.63	3.97	2.49	2.95	19.01	1.79	7.14	0.31
	(0.004)	(0.137)	(0.287)	(0.228)	(0.00)	(0.408)	(0.028)	(0.856)

Notes:

1. BFBN, BFBS, ABEN, PKLN, EMBE, EMBW, LDBN, and LDBS denotes Blackfrairs Bridge North, Blackfrairs Bridge South, Albert Embankment North, Park Lane North, Embankment East, Embankment West, London Bridge North and London Bridge South, respectively.
2. ***p<0.01; **p<0.05, and *p<0.10.
3. Any results which failed the White Test, are already adjusted with Heteroscedasticity-Consistency Standard Errors.
4. Figures in parentheses under the coefficients are ‘t-statistics’ and under the diagnostic tests are ‘p-values’.

Table 3.3.9 Linear Speed-Flow Ordinary Congestion Specification: Dependent Variable *V*

Variables	Coefficients
BFBN	61.143***
	(13.33)
BFBS	56.501***
	(12.55)
AMBN	53.709***
	(13.51)
PKLN	62.002***
	(18.35)
EMBE	58.716***
	(25.67)
EMBW	52.123***
	(30.47)
LDBN	53.354***
	(16.69)
LDBS	-0.049***
	(-3.01)
BFBN_F	-0.049***
	(-3.01)
BFBS_F	-0.015
	(-1.39)
AMBN_F	-0.013***
	(-1.53)
PKLN_F	-0.010***
	(-3.85)
EMBE_F	-0.007***
	(-2.53)
EMBW_F	-0.007***
	(-2.66)
LDBN_F	-0.013*
	(-1.84)
LDBS_F	-0.017
	(-1.33)

Diagnostic Statistics	
Observations	416
F-Statistics	1031.02
Adjusted R^2	0.975
Heteroscedasticity :Chi-Squared	0.84
	(0.360)
White Test:Chi-Squared	0.911
	(0.633)
RESET:F-Statistics	2.68
	(0.046)
Normality:Chi-Squared	9.15
	(0.010)
Testing Restrictions:	
(1) $H_0: \phi_1 = \phi_2 = \phi_3 = \phi_4 = \phi_5 = \phi_6 = \phi_7 = \phi_8$	1.71
	(0.105)
(2) $H_0: \varphi_1 = \varphi_2 = \varphi_3 = \varphi_4 = \varphi_5 = \varphi_6 = \varphi_7 = \varphi_8$	1.20
	(0.299)

Notes:

1. BFBN, BFBS, ABEN, PKLN, EMBE, EMBW, LDBN, and LDBS denotes Blackfrairs Bridge North, Blackfrairs Bridge South, Albert Embankment North, Park Lane North, Embankment East, Embankment West, London Bridge North and London Bridge South, respectively.
2. ***p<0.01; **p<0.05, and *p<0.10.
3. Figures in parentheses under the coefficients are ‘t-statistics’ and under the diagnostic tests are ‘p-values’.

Table 3.3.10 Linear Speed-Flow Specification: Dependent Variable *V*

Variables	Coefficients
BFBN	50.478***
	(34.66)
BFBS	54.243***
	(29.21)
AMBN	52.121***
	(31.45)
PKLN	60.620***
	(26.28)
EMBE	60.136***
	(44.00)
EMBW	53.443***
	(48.03)
LDBN	51.766***
	(42.87)
LDBS	54.971***
	(26.26)
F	-0.009***
	(-6.18)

Diagnostic Statistics	
Observations	416
F-Statistics	1825.57
Adjusted R^2	0.975
Heteroscedasticity :Chi-Squared	1.10
	(0.293)
White Test:Chi-Squared	1.20
	(0.548)
RESET:F-Statistics	3.03
	(0.029)
Normality:Chi-Squared	7.61
	(0.022)
Testing Restrictions:	
(1) H_0: $\phi_1=\phi_2=\phi_3=\phi_4=\phi_5=\phi_6=\phi_7=\phi_8$	8.99
	(0.000)

Notes:

1. BFBN, BFBS, ABEN, PKLN, EMBE, EMBW, LDBN, and LDBS denotes Blackfrairs Bridge North, Blackfrairs Bridge South, Albert Embankment North, Park Lane North, Embankment East, Embankment West, London Bridge North and London Bridge South, respectively.
2. ***p<0.01; **p<0.05, and *p<0.10.
3. Figures in parentheses under the coefficients are ‘t-statistics’ and under the diagnostic tests are ‘p-values’.

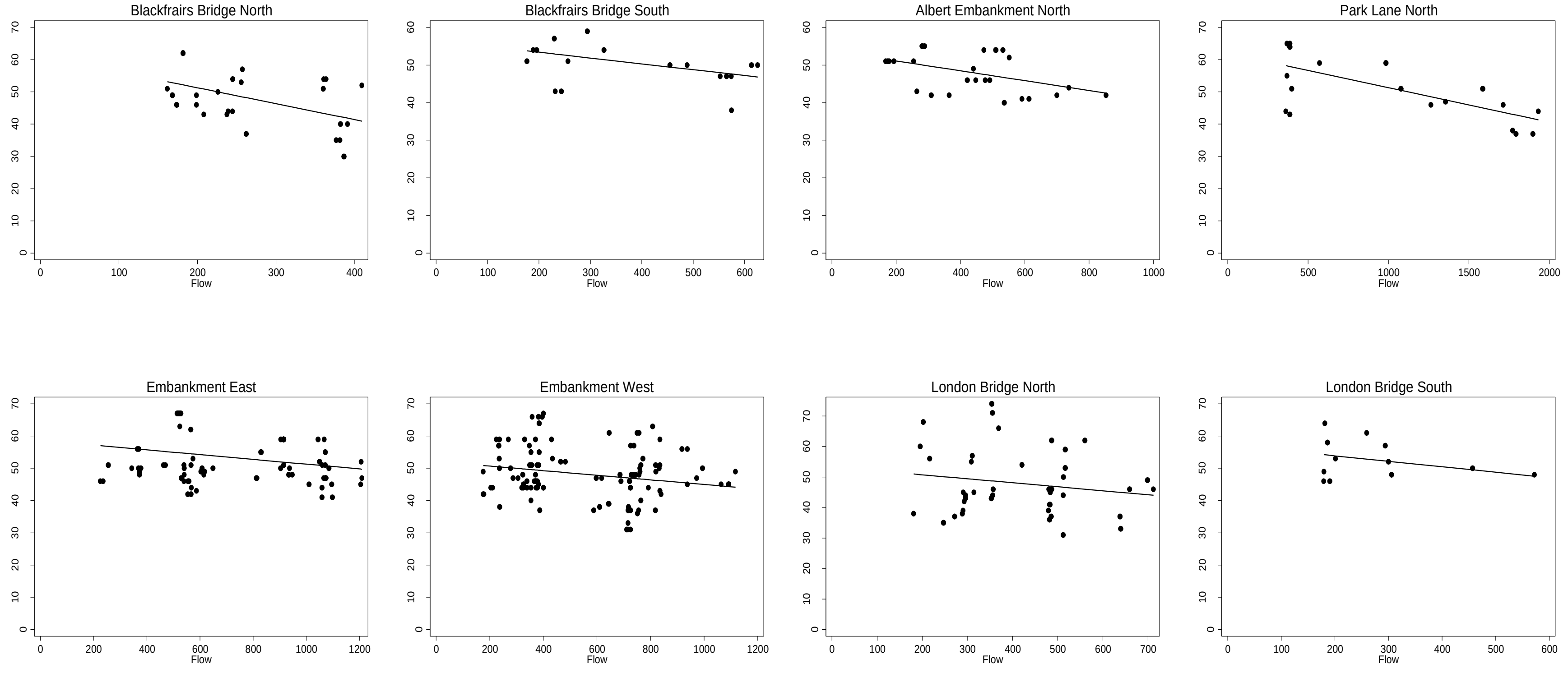

Figure 3.3.9 Speed-Flow Observations with Predicted Speeds Corresponding to Table 3.3.8 [V vs F: using street data]

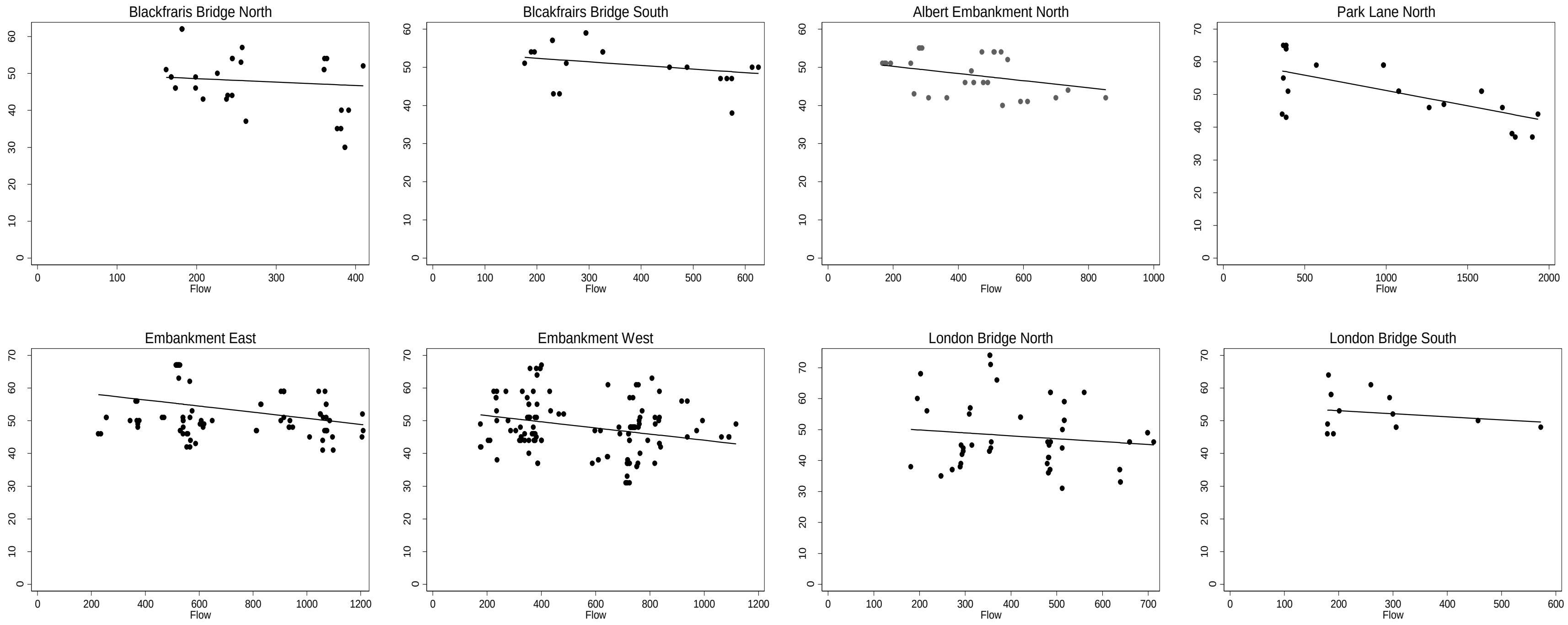

Figure 3.3.10 Speed-Flow Observations with Predicted Speeds Corresponding to Table 3.3.10 [V vs F: using the street data aggregation]

Secondly, we consider a quadratic model using (3.3.4)

$$V = \psi + \xi F + \Omega (F)^2 + \delta \qquad (3.3.4)$$

where *V* represents car speeds and *F* represents traffic flows.

The corresponding results and their diagnostic statistics are presented in Table 3.3.11. The results show that less than a quarter of the estimated coefficients for the linear and quadratic variables are statistically significantly different from zero with 90% significance level and only about half of the regressions pass the RESET and Normality tests. The predicted speeds corresponding to these regressions are shown in Figure 3.3.11.

Next, we adjust the specification by aggregating all observations of eight streets into a single data set. In order to check whether we can use the same simple linear model for eight streets, we add dummy variables. In addition to the diagnostic tests, we test equality in each intercept, slope and curvature terms. The results show that we cannot reject three hypotheses of equality in each of intercept, slope and curvature terms in Table 3.3.12 and two restrictions of equality in each of intercept and slope terms in Table 3.3.13. Therefore, the final regression of aggregated data set is shown in Table 3.3.14; which rejects the restriction of equality in intercept terms. Additionally, eight predicted speeds corresponding to this regression are shown in Figure 3.3.12. The slopes of the relationships are mainly negative but not statistically significant.

Table 3.3.11 Quadratic Speed-Flow Specifications: Dependent Variable *V*

Variables	BFBN	BFBS	AMBN	PKLN	EMBE	EMBW	LDBN	LDBS
Constant	56.960**	47.942***	51.274***	54.489***	42.152***	55.847***	48.150***	55.158***
	(2.46)	(4.43)	(10.02)	(8.00)	(11.35)	(15.42)	(3.79)	(6.55)
F	-0.016	0.035	$-5.94x10^{-4}$	0.009	0.043***	-0.021*	0.013	-0.004
	(-0.09)	(0.57)	(-0.03)	(0.74)	(3.45)	(-1.68)	(0.22)	(-0.10)
$(F)^2$	$-5.74x10^{-5}$	$-6.33x10^{-5}$	$-1.35x10^{-5}$	$-9.20x10^{-6}$*	$-3.45x10^{-5}$***	$1.22x10^{-5}$	$-2.99x10^{-5}$	$1.52x10^{-5}$
	(-0.18)	(-0.82)	(-0.54)	(-1.80)	(-3.80)	(1.16)	(-0.44)	(-0.35)
Diagnostic Statistics								
Observations	32	20	27	23	97	142	60	15
F-Statistics	4.47	2.63	3.28	11.68	7.40	0.27	0.95	1.66
Adjusted R^2	0.183	0.146	0.149	0.492	0.117	0.046	0.001	0.216
Heteroscedasticity :Chi-Squared	1.19	0.13	0.09	2.59	13.53	0.27	2.72	2.03
	(0.275)	(0.714)	(0.766)	(0.107)	(0.000)	(0.600)	(0.099)	(0.153)
White Test:Chi-Squared	4.22	1.22	4.13	5.47	38.20	1.48	4.098	4.694
	(0.120)	(0.541)	(0.126)	(0.064)	(0.000)	(0.474)	(0.128)	(0.095)
RESET:F-Statistics	7.36	0.99	0.22	0.95	2.01	3.51	1.39	0.39
	(0.001)	(0.426)	(0.881)	(0.437)	(0.117)	(0.017)	(0.254)	(0.760)
Normality:Chi-Squared	9.71	4.23	2.91	1.34	14.19	2.79	4.92	0.42
	(0.007)	(0.120)	(0.233)	(0.511)	(0.000)	(0.248)	(0.085)	(0.810)

Notes:

1. BFBN, BFBS, ABEN, PKLN, EMBE, EMBW, LDBN, and LDBS denotes Blackfrairs Bridge North, Blackfrairs Bridge South, Albert Embankment North, Park Lane North, Embankment East, Embankment West, London Bridge North and London Bridge South, respectively.
2. ***p<0.01; **p<0.05, and *p<0.10.
3. Any results which failed the White Test, are already adjusted with Heteroscedasticity-Consistency Standard Errors.
4. Figures in parentheses under the coefficients are ‘t-statistics’ and under the diagnostic tests are ‘p-values’.

Table 3.3.12 Quadratic Speed-Flow Specification: Dependent Variable *V*

Variables	Coefficients
BSBN	56.96***
	(2.49)
BFBS	47.94***
	(2.88)
AMBN	51.27***
	(6.16)
PKLN	54.48***
	(7.90)
EMBE	42.15***
	(6.12)
EMBW	55.84***
	(14.94)
LDBN	48.15***
	(5.34)
LDBS	55.15***
	(4.58)
BFBN_F	-0.016
	(-0.10)
BFBS_F	0.035
	(0.37)
AMBN_F	-0.001
	(-0.02)
PKLN_F	0.009
	(0.57)
EMBE_F	0.043**
	(2.16)
EMBW_F	-0.021*
	(-1.63)
LDBN_F	0.013
	(0.31)
LDBS_F	-0.004
	(-0.06)
$BFBN(F)^2$	-5.74×10^{-5}
	(-0.19)
$BFBS(F)^2$	-6.33×10^{-5}
	(-0.53)
$AMBN(F)^2$	-1.35×10^{-5}
	(-0.33)
$PKLN(F)^2$	-9.20×10^{-6}
	(-1.25)
$EMBE(F)^2$	-3.45×10^{-5}***
	(-2.55)
$EMBW(F)^2$	1.22×10^{-5}
	(1.12)
$LDBN(F)^2$	-2.99×10^{-5}
	(-0.62)
$LDBS(F)^2$	-1.52×10^{-5}
	(-0.19)

Diagnostic Statistics	
Observations	416
F-Statistics	691.45
Adjusted R^2	0.976
Heteroscedasticity :Chi-Squared	0.70
	(0.402)
White Test:Chi-Squared	0.770
	(0.680)
RESET:F-Statistics	0.12
	(0.947)
Normality:Chi-Squared	8.93
	(0.011)
Testing Restrictions:	
(1) $H_0:\psi_1=\psi_2=\psi_3=\psi_4=\psi_5=\psi_6=\psi_7=\psi_8$	0.51
	(0.828)
(2) $H_0:\xi_1=\xi_2=\xi_3=\xi_4=\xi_5=\xi_6=\xi_7=\xi_8$	1.11
	(0.353)
(3) $H_0:\Omega_1=\Omega_2=\Omega_3=\Omega_4=\Omega_5=\Omega_6=\Omega_7=\Omega_8$	1.11
	(0.356)

Notes:

1. BFBN, BFBS, ABEN, PKLN, EMBE, EMBW, LDBN, and LDBS denotes Blackfrairs Bridge North, Blackfrairs Bridge South, Albert Embankment North, Park Lane North, Embankment East, Embankment West, London Bridge North and London Bridge South, respectively.
2. ***p<0.01; **p<0.05, and *p<0.10.
3. Figures in parentheses under the coefficients are 't-statistics' and under the diagnostic tests are 'p-values'.

Table 3.3.13 Quadratic Speed-Flow Specification: Dependent Variable *V*

Variables	Coefficients
BFBN	60.52***
	(13.17)
BFBS	55.36***
	(12.15)
AMBN	52.19***
	(12.76)
PKLN	55.12***
	(9.86)
EMBE	54.67***
	(15.73)
EMBW	49.54***
	(20.75)
LDBN	51.88***
	(15.58)
LDBS	56.10***
	(12.65)
BFBN_F	-0.044***
	(-2.68)
BFBS_F	-0.008
	(-0.73)
AMBN_F	-0.005
	(-0.54)
PKLN_F	0.007
	(0.62)
EMBE_F	0.005
	(0.59)
EMBW_F	0.003
	(0.43)
LDBN_F	-0.005
	(-0.66)
LDBS_F	-0.009
	(0.73)
$(F)^2$	-8.36×10^{-6}
	(-1.54)

Diagnostic Statistics	
Observations	416
F-Statistics	973.86
Adjusted R^2	0.976
Heteroscedasticity :Chi-Squared	0.63
	(0.428)
White Test:Chi-Squared	1.081
	(0.582)
RESET:F-Statistics	0.82
	(0.482)
Normality:Chi-Squared	8.71
	(0.012)
Testing Restrictions:	
(1) $H_0: \psi_1 = \psi_2 = \psi_3 = \psi_4 = \psi_5 = \psi_6 = \psi_7 = \psi_8$	1.23
	(0.286)
(2) $H_0: \xi_1 = \xi_2 = \xi_3 = \xi_4 = \xi_5 = \xi_6 = \xi_7 = \xi_8$	1.50
	(0.166)

Notes:

1. BFBN, BFBS, ABEN, PKLN, EMBE, EMBW, LDBN, and LDBS denotes Blackfrairs Bridge North, Blackfrairs Bridge South, Albert Embankment North, Park Lane North, Embankment East, Embankment West, London Bridge North and London Bridge South, respectively.
2. ***p<0.01; **p<0.05, and *p<0.10.
3. Figures in parentheses under the coefficients are ‘t-statistics’ and under the diagnostic tests are ‘p-values’.

Table 3.3.14 Quadratic Speed-Flow Specification: Dependent Variable *V*

Variables	Coefficients
BFBN	49.924***
	(28.79)
BFBS	53.564***
	(24.48)
AMBN	51.382***
	(24.69)
PKLN	60.383***
	(25.77)
EMBE	59.285***
	(29.78)
EMBW	52.619***
	(29.41)
LDBN	51.015***
	(29.02)
LDBS	54.392***
	(223.50)
F	-0.006
	(-1.48)
$(F)^2$	$-1.68\text{x}10^{-6}$
	(-0.59)

Diagnostic Statistics	
Observations	416
F-Statistics	1640.41
Adjusted R^2	0.975
Heteroscedasticity :Chi-Squared	1.03
	(0.309)
White Test:Chi-Squared	1.17
	(0.555)
RESET:F-Statistics	3.03
	(0.029)
Normality:Chi-Squared	7.50
	(0.023)
Testing Restrictions:	
(1) $H_0 : \psi_1 = \psi_2 = \psi_3 = \psi_4 = \psi_5 = \psi_6 = \psi_7 = \psi_8$	8.98
	(0.000)

Notes:

1. BFBN, BFBS, ABEN, PKLN, EMBE, EMBW, LDBN, and LDBS denotes Blackfrairs Bridge North, Blackfrairs Bridge South, Albert Embankment North, Park Lane North, Embankment East, Embankment West, London Bridge North and London Bridge South, respectively.
2. ***p<0.01; **p<0.05, and *p<0.10.
3. Figures in parentheses under the coefficients are ‘t-statistics’ and under the diagnostic tests are ‘p-values’.

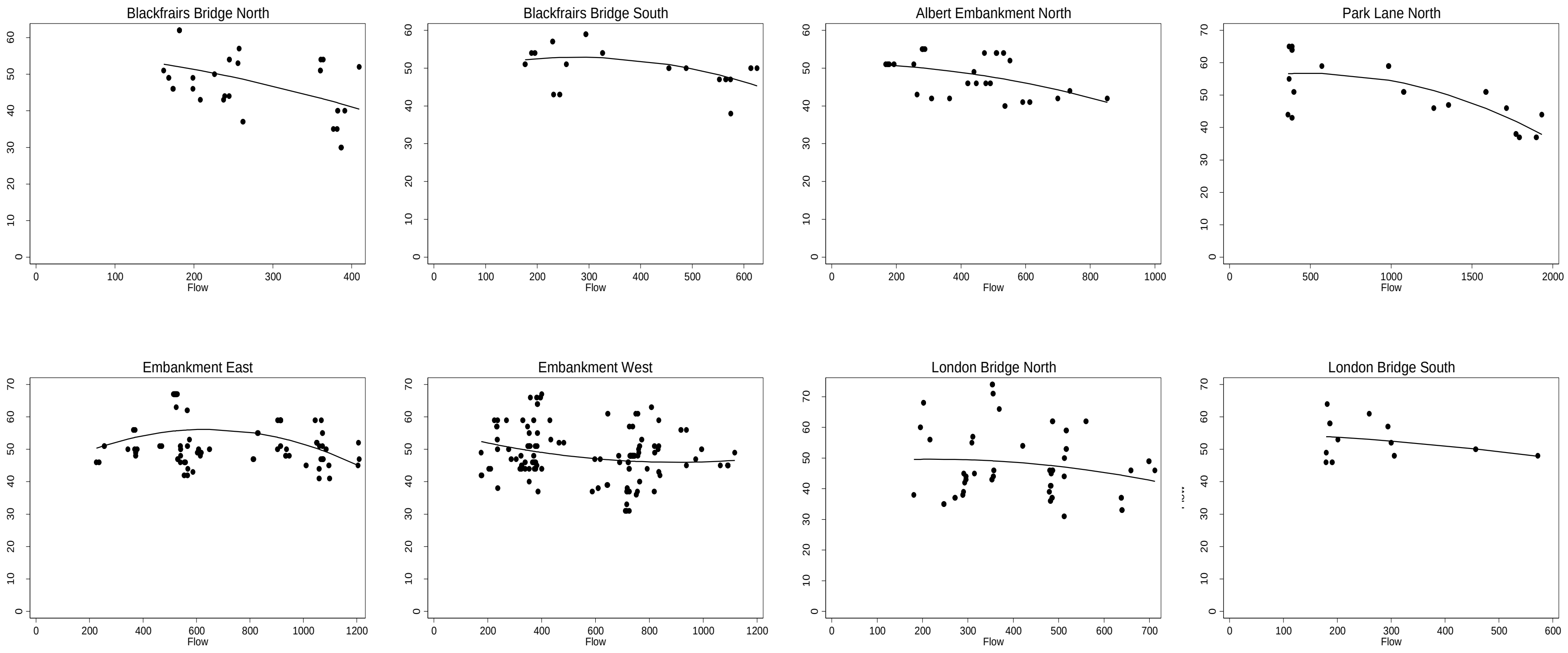

Figure 3.3.11 Speed-Flow Observations with Predicted Speeds Corresponding to Table 3.3.11 [V vs F F^2 : using street data]

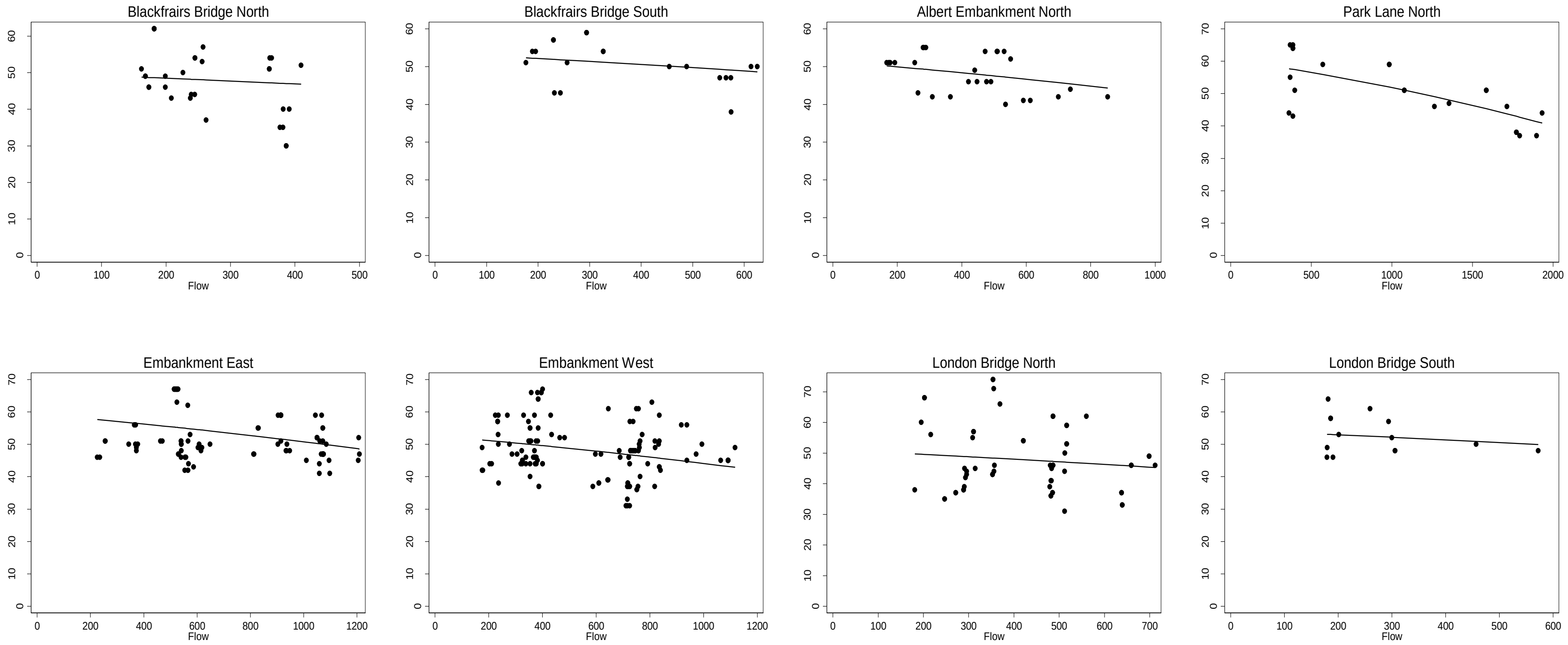

Figure 3.3.12 Speed-Flow Observations with Predicted Speeds Corresponding to Table 3.3.14 [V vs F F^2 : using street data]

Thirdly, we examine the speed-flow relationships with a SPLINE regression in logs specification with one knot.

$$lnV = \alpha + \beta_1 \, lnF1 + \beta_2 \, lnF2 + \varepsilon \qquad (3.3.5)$$

where *V* represents car speeds and *F1 and F2* represent traffic flows before and after a knot, respectively. Accordingly, we estimate a total of three regression parameters i.e. one intercept and two slopes. The knot on each street is chosen at the median flow. Such a SPLINE in logs function is continuous at the knot point.

The results and diagnostic statistics are displayed in Table 3.3.15. The results show that only one quarter of the first slope coefficients are statistically significantly different from zero at 95% confidence level and 50% of them are negative. Whereas three quarters of the second slope coefficients are statistically significant different from zero at 95% confidence level and all but one are negative. Such results might be anticipated as the slope increase from near zero to a more negative value as flow increases. However, only one half of these regressions passed the RESET and Normality diagnostic tests. The predicted speeds are presented in Figure 3.3.13.

Next, we adjust the specification by aggregating all observations of eight streets into a single data set. In order to check whether we can use the same SPLINE in logs model for eight streets; we add intercept and slope dummy variables. In addition to the diagnostic tests, we test equality in each of the intercept and slope terms. The results in Table 3.3.16 show that we cannot reject three hypothesis of equality in each of intercept, slope before a knot and slope after a knot terms. Therefore, the final regression of aggregated data set is shown in Table 3.3.17; which rejects the restriction of equality in intercept terms. Additionally, eight predicted speeds corresponding to this regression are shown in Figure 3.3.14. The SPLINE logarithmic regressions give statistically significant negative slopes for each street.

Table 3.3.15 SPLINE in logs Speed-Flow Specifications: Dependent Variable ln*V*

Variables	BFBN	BFBS	AMBN	PKLN	EMBE	EMBW	LDBN	LDBS
Constant	5.028***	3.115***	4.158***	4.130***	3.249***	4.616***	3.614***	3.498***
	(4.92)	(3.31)	(10.87)	(8.73)	(10.24)	(19.48)	(4.13)	(3.26)
lnF1	-0.208	0.155	-0.044	-0.017	0.121**	-0.124***	0.045	0.090
	(-1.08)	(0.91)	(-0.67)	(-0.24)	(2.28)	(-3.19)	(0.30)	(0.45)
lnF2	-0.362*	-0.227**	-0.243*	-0.559***	-0.207***	0.137	-0.310	-0.200*
	(-1.84)	(-2.43)	(-1.87)	(-3.53)	(-3.26)	(1.07)	(-1.38)	(-1.90)
Diagnostic Statistics								
Observations	32	20	27	23	97	142	60	15
F-Statistics	4.79	3.24	3.52	3.99	5.62	5.31	1.17	2.12
Adjusted R^2	0.196	0.190	0.162	0.502	0.087	0.057	0.005	0.138
Heteroscedasticity :Chi-Square	4.35	0.15	2.10	3.99	15.81	5.19	0.65	2.87
	(0.113)	(0.926)	(0.349)	(0.136)	($1x10^{-4}$)	(0.074)	(0.420)	(0.238)
White Test:Chi-Squared	9.412	0.200	6.471	1.997	34.640	2.008	1.842	2.434
	(0.009)	(0.904)	(0.039)	(0.368)	($3x10^{-8}$)	(0.366)	(0.398)	(0.296)
RESET:F-Statistics	0.49	1.92	0.58	1.39	7.97	5.35	4.49	0.59
	(0.693)	(0.172)	(0.632)	(0.280)	($1x10^{-4}$)	(0.001)	(0.007)	(0.635)
Normality:Chi-Squared	4.23	7.74	2.64	1.59	12.85	0.18	8.18	0.41
	(0.120)	(0.020)	(0.267)	(0.451)	($1.6x10^{-3}$)	(0.913)	(0.016)	(0.816)

Notes:

1. BFBN, BFBS, ABEN, PKLN, EMBE, EMBW, LDBN, and LDBS denotes Blackfrairs Bridge North, Blackfrairs Bridge South, Albert Embankment North, Park Lane North, Embankment East, Embankment West, London Bridge North and London Bridge South, respectively.
2. ***p<0.01; **p<0.05, and *p<0.10.
3. Any results which failed the White Test, are already adjusted with Heteroscedasticity-Consistency Standard Errors.
4. Figures in parentheses under the coefficients are 't-statistics' and under the diagnostic tests are 'p-values'.

Table 3.3.16 SPLINE in Logs Speed-Flow Specification: Dependent Variable ln*V*

Variables	Coefficients
BFBN	5.028***
	(4.10)
BFBS	3.115**
	(2.13)
AMBN	4.158***
	(6.92)
PKLN	4.130***
	(7.20)
EMBE	3.249***
	(5.90)
EMBW	4.616***
	(19.52)
LDBN	3.614***
	(5.80)
LDBS	3.498***
	(2.18)
BFBN_lnF1	-0.208
	(-1.10)
BFBS_lnF1	0.155*
	(1.71)
AMBN_lnF1	-0.044
	(-1.10)
PKLN_lnF1	-0.017
	(-0.26)
EMBE_lnF1	0.121**
	(2.25)
EMBW_lnF1	-0.124***
	(-3.07)
LDBN_lnF1	0.045
	(0.26)
LDBS_lnF1	0.090
	(0.45)
BFBN_lnF2	-0.362*
	(-1.88)
BFBS_lnF2	-0.227***
	(-2.72)
AMBN_lnF2	-0.243***
	(-3.33)
PKLN_lnF2	-0.559***
	(-5.34)
EMBE_lnF2	-0.207***
	(-3.21)
EMBW_lnF2	0.137
	(1.53)
LDBN_lnF2	-0.310
	(-1.58)
LDBS_lnF2	-0.200***
	(-3.59)

Diagnostic Statistics	
Observations	416
F-Statistics	10409.92
Adjusted R^2	0.998
Heteroscedasticity :Chi-Squared	4.69
	(0.030)
White Test:Chi-Squared	6.705
	(0.035)
RESET:F-Statistics	2.10
	(0.099)
Normality:Chi-Squared	2.06
	(0.357)
Testing Restrictions:	
(1) $H_0: \alpha_1 = \alpha_2 = \alpha_3 = \alpha_4 = \alpha_5 = \alpha_6 = \alpha_7 = \alpha_8$	1.15
	(0.333)
(2) $H_0: \beta_{11} = \beta_{12} = \beta_{13} = \beta_{14} = \beta_{15} = \beta_{16} = \beta_{17} = \beta_{18}$	1.34
	(0.228)
(3) $H_0: \beta_{21} = \beta_{22} = \beta_{23} = \beta_{24} = \beta_{25} = \beta_{26} = \beta_{27} = \beta_{28}$	1.71
	(0.105)

Notes:

1. BFBN, BFBS, ABEN, PKLN, EMBE, EMBW, LDBN, and LDBS denotes Blackfrairs Bridge North, Blackfrairs Bridge South, Albert Embankment North, Park Lane North, Embankment East, Embankment West, London Bridge North and London Bridge South, respectively.
2. ***p<0.01; **p<0.05, and *p<0.10.
3. Any results which failed the White Test, are already adjusted with Heteroscedasticity-Consistency Standard Errors.
4. Figures in parentheses under the coefficients are ‘t-statistics’ and under the diagnostic tests are ‘p-values’.

Table 3.3.17 SPLINE in Logs Speed-Flow Specification: Dependent Variable ln*V*

Variables	Coefficients
BFBN	4.196***
	(27.70)
BFBS	4.294***
	(27.50)
AMBN	4.231***
	(25.56)
PKLN	4.328***
	(23.38)
EMBE	4.375***
	(25.22)
EMBW	4.233***
	(24.36)
LDBN	4.208***
	(25.64)
LDBS	4.300***
	(27.88)
lnF1	-0.058**
	(-2.08)
lnF2	-0.179***
	(-4.21)

Diagnostic Statistics	
Observations	416
F-Statistics	24495
Adjusted R^2	0.998
Heteroscedasticity :Chi-Squared	2.21
	(0.137)
White Test:Chi-Squared	2.91
	(0.232)
RESET:F-Statistics	3.04
	(0.028)
Normality:Chi-Squared	1.51
	(0.469)
Testing Restrictions:	
(1) H_0: $\alpha_1=\alpha_2=\alpha_3=\alpha_4=\alpha_5=\alpha_6=\alpha_7=\alpha_8$	8.65
	(0.000)

Notes:

1. BFBN, BFBS, ABEN, PKLN, EMBE, EMBW, LDBN, and LDBS denotes Blackfrairs Bridge North, Blackfrairs Bridge South, Albert Embankment North, Park Lane North, Embankment East, Embankment West, London Bridge North and London Bridge South, respectively.
2. ***p<0.01; **p<0.05, and *p<0.10.
3. Figures in parentheses under the coefficients are 't-statistics' and under the diagnostic tests are 'p-values'.

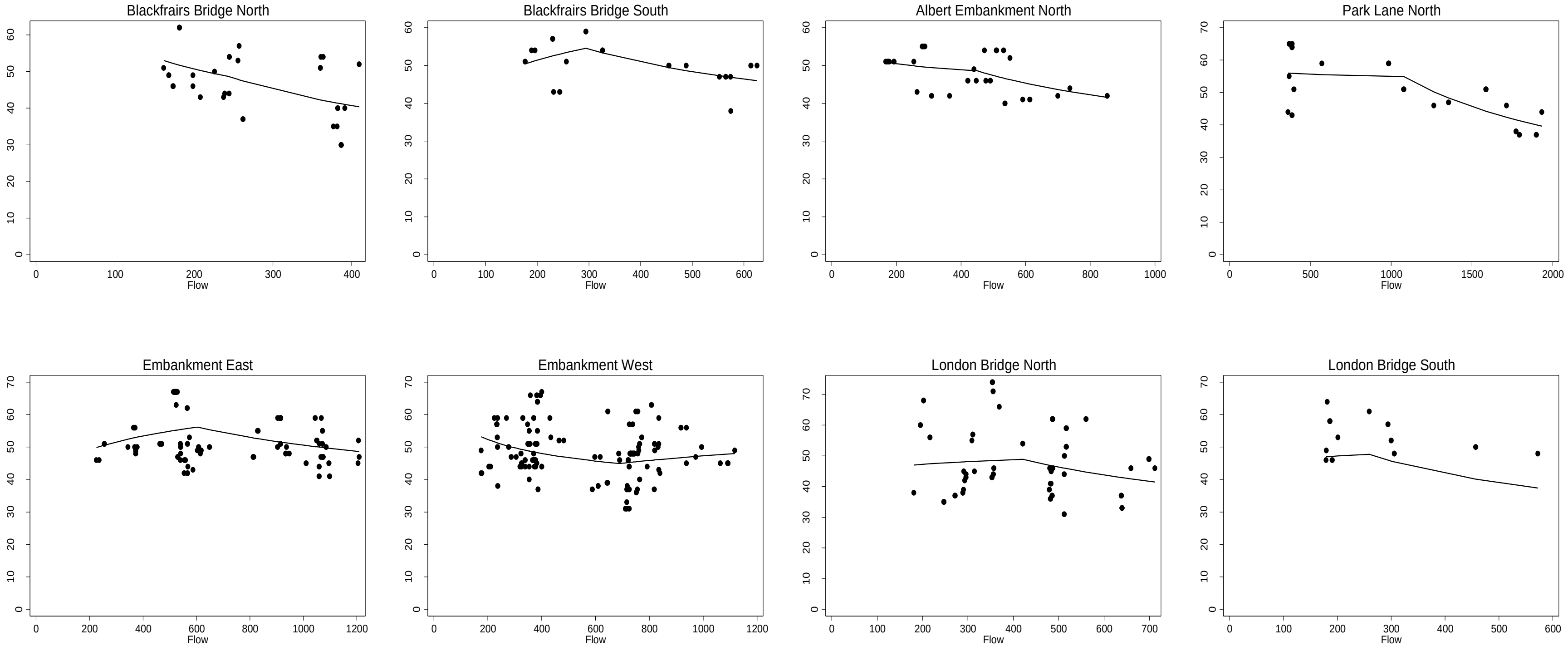

Figure 3.3.13 Speed-Flow Observations with Predicted Speeds Corresponding to Table 3.3.15 [lnV vs lnF1 lnF2: using street data]

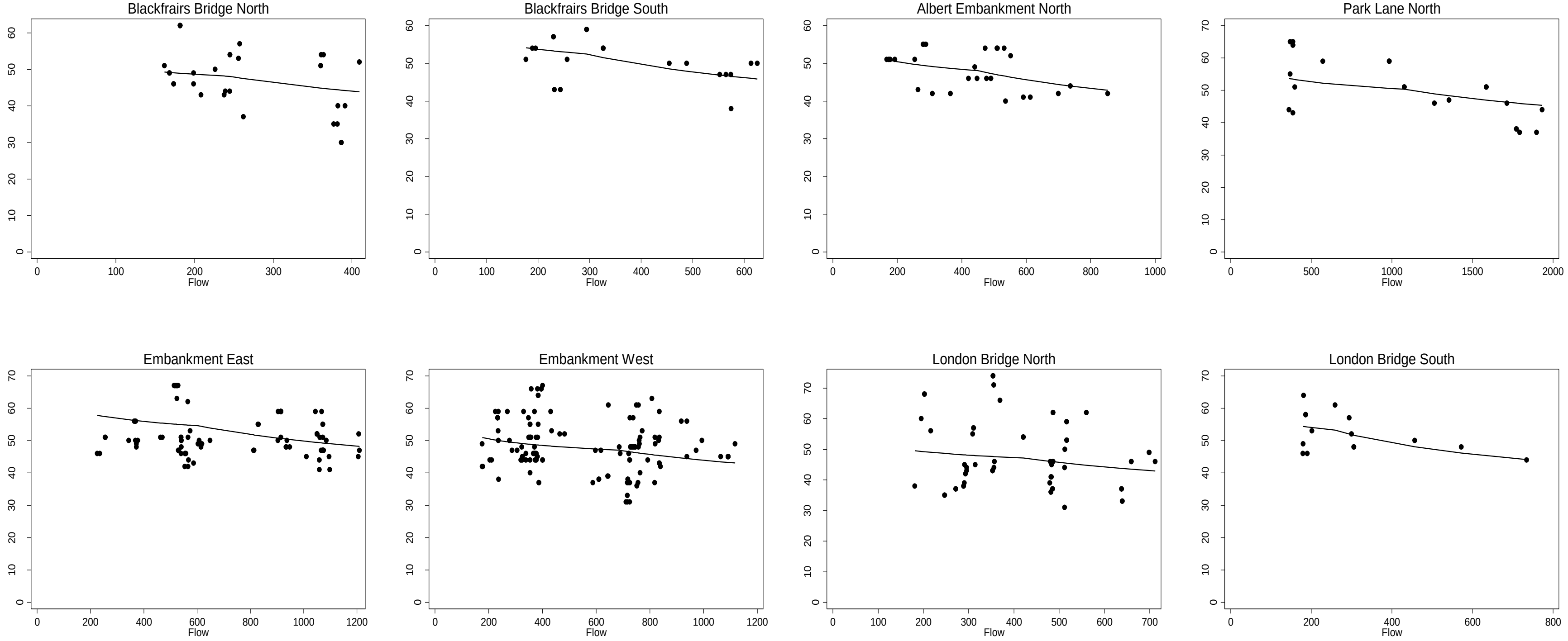

Figure 3.3.14 Speed-Flow Observations with Predicted Speeds Corresponding to Table 3.3.17 [lnV vs lnF1 lnF2: using street data]

Finally, we examine the speed-flow relationships with a simple SPLINE with one knot.

$$V = \phi + \varphi_1 F1 + \varphi_2 F2 + \varepsilon \tag{3.3.6}$$

where V represents car speeds and *F1 and F2* represent traffic flows before and after a knot, respectively.

Accordingly, we estimate a total of three regression parameters, i.e. one intercept and two slopes. Such a linear SPLINE function is continuous at the knot point. The knot on each street is chosen at the median flow. This regression results are used to estimate elasticities and the second elasticity (at higher flow) is expected to be higher than the first.

The results and diagnostic statistics are displayed in Table 3.3.18. The results suggest only one of the first slope coefficients are statistically significantly different from zero at 99% confidence level and 50% of them are negative. Whereas five of the second slope coefficients are statistically significant different from zero at 90% confidence level and all but one are negative. Such results might be anticipated as the slope increases from near zero to a more negative value as flow increases. However, only three of these regressions passed both the RESET and Normality diagnostic tests. The predicted speeds are presented in Figure 3.3.15.

Next, we adjust the specification by aggregating all observations of eight streets into a single data set. In order to check whether we can use the same simple linear SPLINE model for eight streets; we add intercept and slope dummy variables. In addition to the diagnostic tests, we test equality in each of the intercept and slope terms. The results in Table 3.3.19 show that we cannot reject the three hypotheses of equality in each of the intercept, slope before a knot and slope after a knot terms. Therefore, the final regression of aggregated data set is shown in Table 3.3.20; which rejects the restriction of equality in intercept terms. Additionally, eight predicted speeds corresponding to this regression are shown in Figure 3.3.16. The linear SPLINE regressions give a statistically significant negative slope for each street.

Table 3.3.18 Linear SPLINE Speed-Flow Specifications: Dependent Variable *V*

Variables	BFBN	BFBS	AMBN	PKLN	EMBE	EMBW	LDBN	LDBS
Constant	61.843***	44.290***	51.921***	58.143***	48.492***	54.905***	47.766***	51.693***
	(5.28)	(5.24)	(14.35)	(14.52)	(9.28)	(26.21)	(5.93)	(5.01)
F1	-0.052	0.035	-0.007	-0.003	0.013	-0.013***	0.005	0.009
	(-0.94)	(1.05)	(-0.69)	(-0.64)	(1.34)	(-3.40)	(0.21)	(0.20)
F2	-0.047*	-0.027*	-0.019*	-0.017***	-0.014***	0.006	-0.028	-0.021
	(-1.73)	(-2.62)	(-1.83)	(-3.12)	(-3.36)	(0.97)	(-1.36)	(-1.72)
Diagnostic Statistics								
Observations	32	20	27	23	97	142	60	15
F-Statistics	4.46	3.68	3.37	11.35	5.89	6.14	1.21	1.82
Adjusted R^2	0.182	0.219	0.154	0.484	0.092	0.067	0.007	0.105
Heteroscedasticity :Chi-Squared	1.15	0.15	0.11	2.76	17.00	0.05	2.10	1.63
	(0.283)	(0.694)	(0.742)	(0.096)	(0.000)	(0.814)	(0.147)	(0.201)
White Test:Chi-Squared	4.58	0.15	5.00	5.60	40.77	0.08	3.25	3.17
	(0.101)	(0.924)	(0.081)	(0.060)	(0.000)	(0.960)	(0.196)	(0.204)
RESET:F-Statistics	0.67	2.29	0.27	0.33	8.12	2.32	2.91	0.71
	(0.576)	(0.122)	(0.844)	(0.804)	(0.000)	(0.078)	(0.042)	(0.568)
Normality:Chi-Squared	10.92	5.88	3.26	1.46	15.06	3.72	5.21	0.48
	(0.004)	(0.052)	(0.196)	(0.483)	(0.000)	(0.155)	(0.073)	(0.787)

Notes:

1. BFBN, BFBS, ABEN, PKLN, EMBE, EMBW, LDBN, and LDBS denotes Blackfrairs Bridge North, Blackfrairs Bridge South, Albert Embankment North, Park Lane North, Embankment East, Embankment West, London Bridge North and London Bridge South, respectively.
2. ***p<0.01; **p<0.05, and *p<0.10.
3. Any results which failed the White Test, are already adjusted with Heteroscedasticity-Consistency Standard Errors.
4. Figures in parentheses under the coefficients are ‘t-statistics’ and under the diagnostic tests are ‘p-values’.

Table 3.3.19 SPLINE Linear Speed-Flow Specification: Dependent Variable *V*

Variables	Coefficients
BFBN	61.843***
	(5.37)
BFBS	44.290***
	(3.26)
AMBN	51.921***
	(8.81)
PKLN	58.143***
	(12.31)
EMBE	48.492***
	(8.82)
EMBW	54.905***
	(25.16)
LDBN	47.766***
	(8.33)
LDBS	51.693***
	(3.68)
BFBN_F1	-0.052
	(-0.96)
BFBS_F1	0.035
	(0.65)
AMBN_F1	-0.007
	(-0.42)
PKLN_F1	-0.003
	(-0.54)
EMBE_F1	0.013
	(1.28)
EMBW_F1	-0.013***
	(-3.26)
LDBN_F1	0.005
	(0.30)
LDBS_F1	0.009
	(0.15)
BFBN_F2	-0.047*
	(-1.75)
BFBS_F2	-0.027
	(-1.63)
AMBN_F2	-0.191
	(-1.12)
PKLN_F2	-0.017***
	(-2.64)
EMBE_F2	-0.014***
	(-3.19)
EMBW_F2	0.006
	(0.93)
LDBN_F2	-0.028*
	(-1.91)
LDBS_F2	-0.021
	(-1.27)

Diagnostic Statistics	
Observations	416
F-Statistics	695.24
Adjusted R^2	0.975
Heteroscedasticity :Chi-Squared	0.92
	(0.338)
White Test:Chi-Squared	1.34
	(0.510)
RESET:F-Statistics	1.53
	(0.207)
Normality:Chi-Squared	9.61
	(0.008)
Testing Restrictions:	
(1) $H_0: \phi_1 = \phi_2 = \phi_3 = \phi_4 = \phi_5 = \phi_6 = \phi_7 = \phi_8$	0.61
	(0.751)
(2) $H_0: \varphi_{11} = \varphi_{12} = \varphi_{13} = \varphi_{14} = \varphi_{15} = \varphi_{16} = \varphi_{17} = \varphi_{18}$	1.20
	(0.301)
(3) $H_0: \varphi_{21} = \varphi_{22} = \varphi_{23} = \varphi_{24} = \varphi_{25} = \varphi_{26} = \varphi_{27} = \varphi_{28}$	1.68
	(0.112)

Notes:

1. BFBN, BFBS, ABEN, PKLN, EMBE, EMBW, LDBN, and LDBS denotes Blackfrairs Bridge North, Blackfrairs Bridge South, Albert Embankment North, Park Lane North, Embankment East, Embankment West, London Bridge North and London Bridge South, respectively.
2. ***p<0.01; **p<0.05, and *p<0.10.
3. Any results which failed the White Test, are already adjusted with Heteroscedasticity-Consistency Standard Errors.
4. Figures in parentheses under the coefficients are ‘t-statistics’ and under the diagnostic tests are ‘p-values’.

Table 3.3.20 Linear SPLINE Speed-Flow Specification: Dependent Variable *V*

Variables	Coefficients
BFBN	50.028***
	(32.59)
BFBS	53.822***
	(28.15)
AMBN	51.342***
	(27.63)
PKLN	59.168***
	(21.22)
EMBE	59.177***
	(34.53)
EMBW	52.236***
	(30.51)
LDBN	50.995***
	(34.79)
LDBS	54.576***
	(25.54)
F1	-0.006**
	(-2.19)
F2	-0.011***
	(-4.00)

Diagnostic Statistics	
Observations	416
F-Statistics	1642.54
Adjusted R^2	0.975
Heteroscedasticity :Chi-Squared	1.31
	(0.251)
White Test:Chi-Squared	1.50
	(0.470)
RESET:F-Statistics	2.94
	(0.033)
Normality:Chi-Squared	7.06
	(0.029)
Testing Restrictions:	
(1)H_0: $\phi_1=\phi_2=\phi_3=\phi_4=\phi_5=\phi_6=\phi_7=\phi_8$	7.06
	(0.029)

Notes:

1. BFBN, BFBS, ABEN, PKLN, EMBE, EMBW, LDBN, and LDBS denotes Blackfrairs Bridge North, Blackfrairs Bridge South, Albert Embankment North, Park Lane North, Embankment East, Embankment West, London Bridge North and London Bridge South, respectively.
2. ***p<0.01; **p<0.05, and *p<0.10.
3. Any results which failed the White Test, are already adjusted with Heteroscedasticity-Consistency Standard Errors.
4. Figures in parentheses under the coefficients are ‘t-statistics’ and under the diagnostic tests are ‘p-values’.

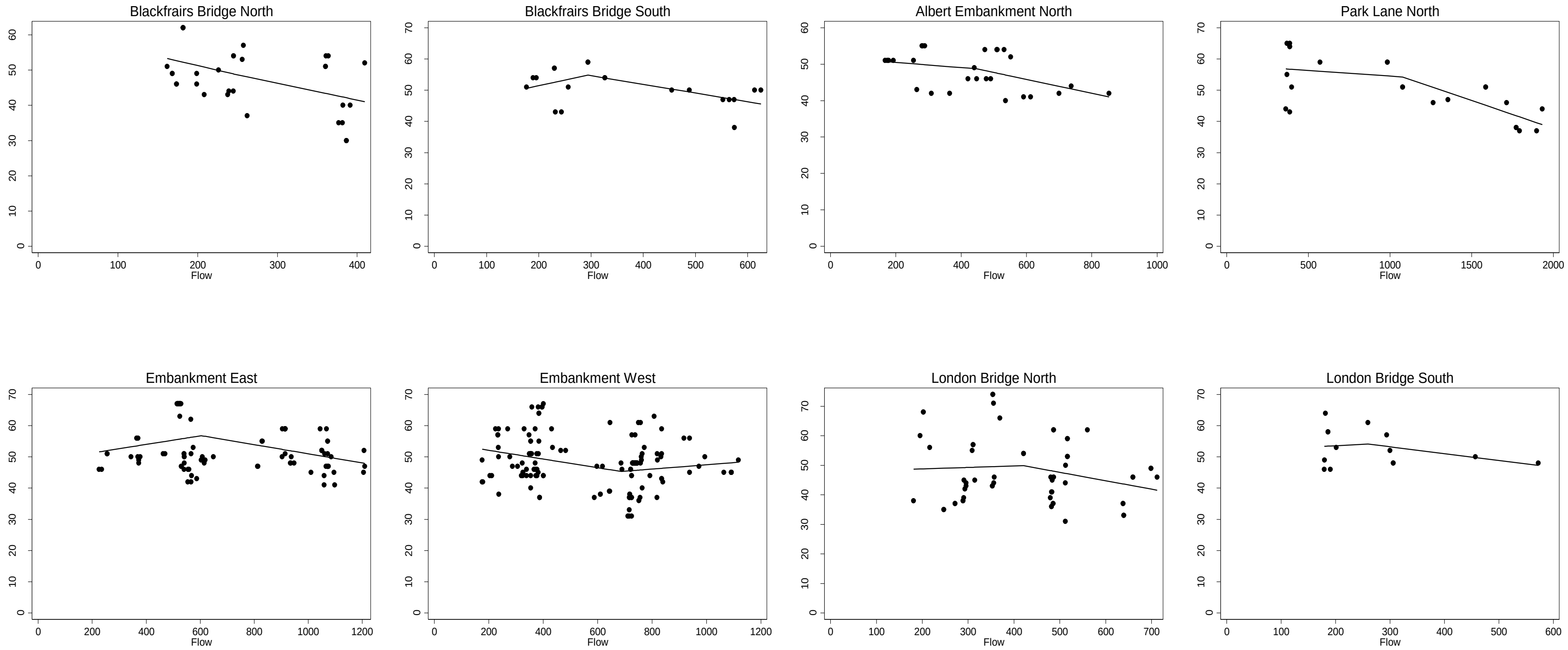

Figure 3.3.15 Speed-Flow Observations with Predicted Speeds Corresponding to Table 3.3.18 [V vs F1 F2: using street data]

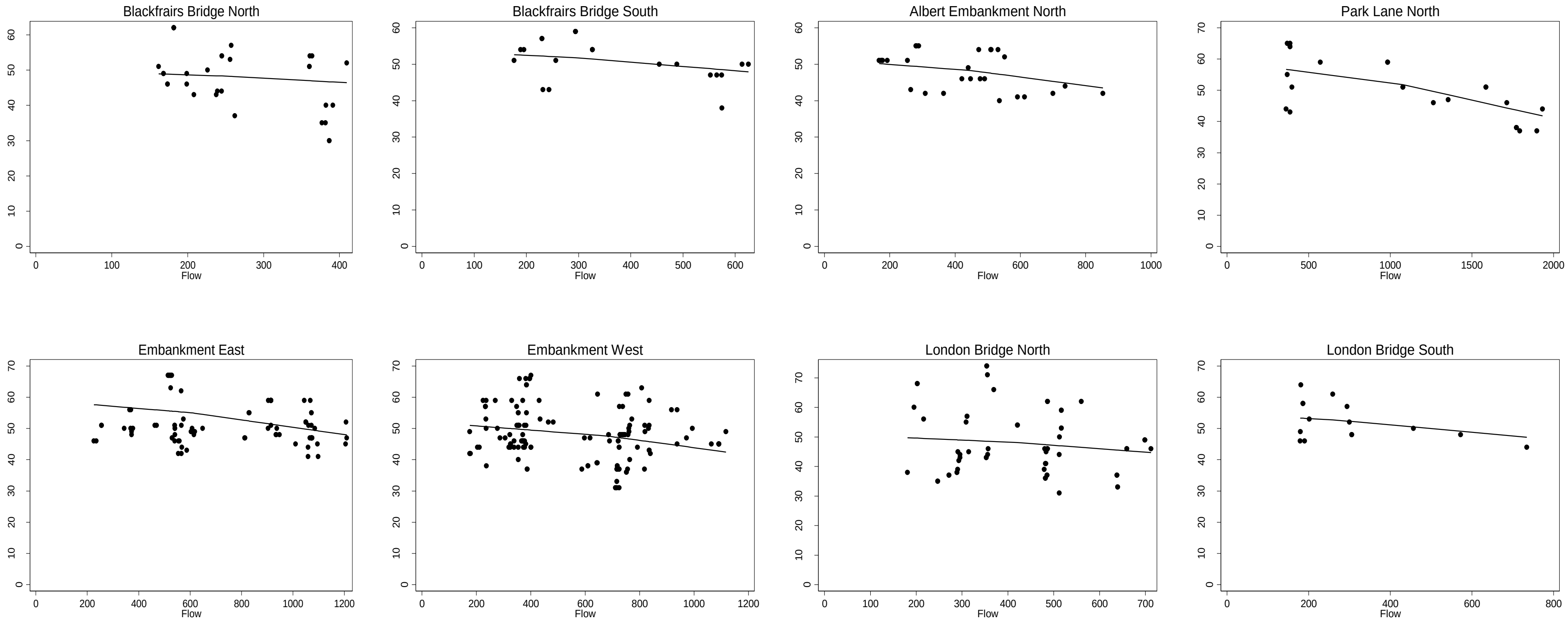

Figure 3.3.16 Speed-Flow Observations with Predicted Speeds Corresponding to Table 3.3.20 [V vs F1 F2: using street data aggregation]

3.4 Discussion of Empirical Results, METCs and Simulations

The statistical evidence presented in this Chapter does not lead to a conclusive view that one regression should be preferred over all others. Thus, in addition to the previous analyses, Table 3.3.21 provides the calculated elasticities of speed with respect to density results from all specifications and data sets. For illustrative purposes, it is useful to identify the median elasticity of speed with respect to density as 0.062 with a large margin of error indicated by the interquartile range of 0.081. The second part of the spline regressions suggest a higher than 0.1 elasticity whilst the other regressions provide lower estimates. As one would expect the slope and elasticity to increase along the top part of the speed/flow relationship and represent a more important congestion effect, one might wish to use the second parts of the spline regressions for illustration of the size of the marginal external time congestion cost. Thus, for the remainder of this Chapter and for illustrative purposes, an elasticity of speed with respect to density of 0.1 is used. We now turn to the estimation of the marginal external congestion time cost using these estimates of the elasticity of speed with respect to density.

The effect of the elasticity of demand with respect to duration of the journey time can be investigated by considering the elasticity of induced demand with respect to journey time. There have been a number of reviews of estimation of this elasticities in different contexts, see Ruiter et al (1979), Pells (1989), Hansen et al (1993), Cohen (1995), Goodwin (1996), Noland and Lem (2000) and Cervero (2001). It is difficult to see a clear and specific consensus amongst these studies, but the immediate elasticity can simply be taken as zero and the short and long run elasticities are taken as -0.5 and -1.0. The meta-analysis by Cervero suggests that these estimates may be slightly on the high side but are given as a conclusion by Goodwin (1996). It should be remembered that the following analysis is for illustrative purposes in considering the impact of this demand effect.

Using the expression (3.2.15), the ordinary congestion marginal external congestion time costs (METCs) are estimated assuming an average speed of 30 km/h,[16] an elasticity of speed with respect to density of -0.1 and the above demand elasticities. These METCs are 0.22, 0.21 and 0.20 minutes per vkm for the three respective demand elasticities. As the first estimate corresponds arithmetically to the conventional method of estimating the METC, these new estimates suggest that the this new method makes little difference to the knowledge of the external costs of congestion, the magnitude of change in the estimates being at most in the order of 10%.

However, the effects of the externality are not fully captured by these estimates for two reasons. Firstly, the elasticity of speed with respect to density is low and does not capture the impact of the new method of estimation around the turning point of the speed flow relation where the elasticity of speed with respect to density is approximately (negative) one by definition. The discussion of the data earlier in this Chapter and the Figure 3.3.2 suggest that the majority of the overall data is around the turning point or during a period of actual hypercongestion. Thus, it is important to investigate the outcomes of the new method for the elasticities occurring just before periods of hypercongestion. Secondly, it is necessary to consider how the estimation of METCs varies when using a method that takes

[16] This speed of 30kmh is consistent with the average speeds in London during periods of ordinary congestion, eg night-time hours, Transport for London (2008). It differs from the night-time speeds depicted in Figure 3.3.4 which are higher as they are speeds recorded in the mid-parts of streets where traffic is less likely to be moving slowly or be stationary.

Table 3.3.21 Elasticities of Speed with Respect to Density and with Respect to Flow

	lnVvslnF		lnV vs lnF $(\ln F)^2$		V vs F		V vs F F^2		SPLINE: lnV vs lnF1 lnF2				SPLINE: V vs F1 F2			
									Slope 1		Slope 2		Slope 1		Slope 2	
Streets	ε_{VD}	ε_{VF}	ε_{VD}	ε_{VF}	ε_{VD}	ε_{VF}	ε_{VD}	ε_{VF}	ε_{VD}	ε_{VF}	ε_{VD}	ε_{VF}	ε_{VD}	ε_{VF}	ε_{VD}	ε_{VF}
BFBN	-0.0403	-0.0420	-0.2269	-0.2935	-0.0478	-0.0502	-0.0370	-0.0384	-0.0554	-0.0587	-0.1521	-0.1794	-0.0258	-0.0265	-0.0110	-0.0111
BFBS	-0.0403	-0.0420	-0.0895	-0.0983	-0.0548	-0.0580	-0.0438	-0.0458	-0.0554	-0.0587	-0.1521	-0.1794	-0.0295	-0.0304	-0.1092	-0.1226
AMBN	-0.0403	-0.0420	-0.1117	-0.1257	-0.0747	-0.0807	-0.0626	-0.0668	-0.0554	-0.0587	-0.1521	-0.1794	-0.0389	-0.0405	-0.1269	-0.1454
PKLN	-0.0403	-0.0420	-0.1634	-0.1953	-0.1587	-0.1887	-0.1671	-0.2006	-0.0554	-0.0587	-0.1521	-0.1794	-0.0677	-0.0726	-0.3098	-0.4489
EMBE	-0.0403	-0.0420	-00819	-0.0892	-0.1095	-0.1230	-0.1035	-0.1154	-0.0554	-0.0587	-0.1521	-0.1794	-0.0566	-0.0600	-0.1830	-0.2240
EMBW	-0.0403	-0.0420	-00952	-0.1052	-0.0995	-0.1105	-0.0892	-0.0979	-0.0554	-0.0587	-0.1521	-0.1794	-0.0485	-0.0510	-0.1701	-0.2050
LDBN	-0.0403	-0.0420	-00946	-0.1044	-0.0740	-0.0799	-0.0619	-0.0659	-0.0554	-0.0587	-0.1521	-0.1794	-0.0394	-0.0410	-0.1239	-0.1414

account of the congestion effects being a dynamic process that occurs across a number of periods. In particular, such an analysis will take account of differences in speeds in which “lost kilometres” are made up in the congestion process.

Analysing the impact of the new method for elasticities of speed with respect to density approaching (negative) one, the asymptotic METCs are infinity, 4 and 2. (for purposes of comparison, the speed is taken again as 30kmh). The dramatic reduction in the METC across these three estimates is caused by the net increase in vkm being reduced by the demand effect consequent on the increase in journey time. In the limit, the METC is reduced to a time that is just determined by the elasticity of demand with respect to journey time and the average speed (measured in kilometres per minute). In the circumstances of a higher elasticity of speed with respect to density, the new method does result in substantial changes in the estimated METCs. For the more realistic example of an elasticity of speed with respect to density of negative one half, the associated METCs are respectively 2, 1.33 and 1.0 which represent important changes associated with this new method, ie a 50% reduction between the conventional method of calculating the METC and the method suggested here for the long run METC.

The following empirical analysis of the METC takes account of the external effect taking place across time and implies a consequent variation in speeds and size of the congestion effect. The analysis was constructed on an Excel database and is listed as file CONGSIMUL and under worksheet LONCONG. The first dynamic effect to consider is that very few journeys are one kilometre or infinitesimally small. For most journeys, there will be a different external effect generated at the beginning and end of the journey because of changes in the speed at these two points. In order to allow for the fact that all journeys are a non-zero finite distance, we assume that all journeys in Central London are of the same distance at 8.21 km., which is the reported average trip distance, see Transport for London (2008). The same reference is used to provide estimates of the average speed at the mid hour points in Table 3.3.22. The negative elasticities of speed with respect to density are assumed as 0.1, 0.5 and 1.0 respectively during hours of ordinary congestion, the hours immediately before or after periods of hyper congestion and in hours of hypercongestion. The first estimate of 0.1 is justified by the previous econometric investigation. The last unitary estimate is considered and justified in the next Chapter. The final estimate is an appropriate guess at the average elasticity between the hours of ordinary congestion and hypercongestion.

Considering a journey of this standard length of 8.21km by one additional user, the effect on all other users on the road at this time is to take a little longer to make their journey. Assuming this happens at the end of the of the other users' journey, the average point of the additional time spent on these journeys occurs at the end time point of the marginal user's journey (assumed to be equal to the average journey distance). This dynamic effect may be important as the longer the journey in distance and the lower the speed, the longer interval between the cause of the external effect (the presence of the additional vehicle) and the actual additional external cost occurring (the value of the time taken to complete the journey by rod users on whom the external cost is imposed). Thus, if speeds and elasticities change over such intervals, this effect may be important. The simulation model allows for such effects and calculates the external effects generated across time.[17]

The longer journey times by all other users in turn cause more other users to spend longer on their journeys. As the former increase in journey times is of a very

[17] By comparison, the conventional analysis assumes that the full external effect occurs instantaneously.

small duration and if the latter take place at the end of the journey, the average point of the latter is a duration of one average journey length from the marginal user starting. The following effects of the infinite regress occur at an average one half times the average journey length from the previous effect.

It might be expected that with no large changes in speed, the impact of this full dynamic analysis would be limited. In particular, for periods of little change in speed and low nearly fixed elasticity of speed with respect to density, the conventional and new methods of estimating the METC differ by little. Thus, the impacts on estimation of METCs is minimal when allowing for the length of average journey distance, the overlapping of the external effect into other time periods and differences between the very short, short and long run demand deterred based estimates of the METC. However, as speeds fall markedly and the elasticity approaches (negative) one, the impact of the dynamic analysis becomes important. These outcomes are clearly visible in Table 3.3.22 for the METCs estimated at the mid-hour points.

For periods of high ordinary congestion and high elasticity of speed with respect to density, the METC is likely to be much higher than for simple periods of ordinary congestion with low elasticity and nearly fixed elasticities of speed with respect to density and high and relatively stable speeds. These effects are modelled with the external effects being generated across time in the simulation model and with high elasticities of speed with respect to density the congestion does not die away quickly as is the case at low elasticities. This effect is seen in Table 3.3. 22 for the METCs at the times of 07.30 and 19.30. The congestion effect dieing away or persisting at low and high elasticities of speed with respect to density respectively is predicted by the equation (3.2.16).

The new method of estimation of the METC explains the generation of external effect in periods of hypercongestion. In periods of hypercongestion, the elasticity of speed with respect to density is equal to or exceeds negative one and the congestion process does not diminish and with an elasticity of one or greater explodes. Thus, further rounds of the external effect can only diminish during periods of ordinary congestion. Consequently, the METC is much higher at the beginning of a period of hypercongestion than at the end of the hypercongestion period. These outcomes are again clearly visible in Table 3.3.22.

Perhaps the most interesting feature of the Table 3.3.22 is that the estimates of METC vary for different amounts of deterred demand adjustments. Thus, a first best policy of correcting for congestion externality has to deal with the difficult problem of which estimates to use to set optimal externality Pigovian taxes. This is a problem without a complete answer and not one previously identified in the economics of road congestion literature.

Table 3.3.22 Estimates of the Marginal External Time Congestion Cost for Central London

Hour	Type of Cong'n	Average speed km/h	$METC_{vsr}$ min/vkm	$METC_{sr}$ min/km	$METC_{lr}$ min/km
0.00	OC	30.00	0.22	0.21	0.20
1.00	OC	30.00	0.22	0.21	0.20
2.00	OC	30.00	0.22	0.21	0.20
3.00	OC	30.00	0.22	0.21	0.20
4.00	OC	30.00	0.22	0.21	0.20
5.00	OC	30.00	0.23	0.22	0.21
6.00	OC	24.90	0.29	0.27	0.26
7.00	OC	19.80	22.47	5.33	3.02
8.00	HC	14.70	154.94	9.40	4.84
9.00	HC	14.27	142.37	9.34	4.83
10.00	HC	13.83	129.40	9.28	4.81
11.00	HC	13.40	116.01	9.21	4.79
12.00	HC	12.97	102.20	9.11	4.77
13.00	HC	12.97	88.37	8.98	4.73
14.00	HC	13.40	74.88	8.21	4.69
15.00	HC	13.63	61.65	8.61	4.62
16.00	HC	13.85	48.64	8.29	4.53
17.00	HC	14.08	35.82	7.82	4.39
18.00	HC	14.30	23.42	7.01	4.12
19.00	HC	17.44	9.58	4.89	3.29
20.00	OC	20.58	2.55	1.73	1.31
21.00	OC	23.72	0.27	0.25	0.24
22.00	OC	26.86	0.24	0.23	0.22
23.00	OC	30.00	0.22	0.21	0.20

If a road user could be identified as only using the road once, then it would be appropriate to charge the very short run marginal external cost as no demand adjustment would be expected. If a road user could be identified as using the road repeatedly and in a habitual manner, then one would expect some adjustment through deterred demand. This may suggest that a tax is charged taking account of the deterred demand adjustment. However, such a charge should vary across time and needs to take account of the time period over which adjustment takes place and the signalling effect of any charge/tax in relation to deterred demand adjustment. Additionally, it is not clear how one could distinguish between different types of road users, ie random and habitual road users. Alternatively, the impact of habitual and random road users in any one period is the same. Consequently, both from a practical and political point of view, it might be thought difficult to treat them differently with regards to implementing different charges. These issues, though important, are complex and difficult to analyse thoroughly and a full analysis lies beyond the scope of this thesis. However, a final point is that this simple brief analysis suggests that habitual repeat road users could be charged less per unit of road use. This would be an argument for discounts for users who make repeat habitual journeys, eg commuters who use the Dartford crossing..

3.5 Conclusions

A different theory and model of the marginal external cost of congestion is developed. This model clarifies the economic cause of congestion and shows how the marginal externality can be estimated from data on only traffic speeds and flows and shows the perhaps surprising importance of the elasticity of demand for transport with respect to journey time in determining the external congestion effect.

Importantly, the degree of difference with the traditional analysis of the congestion externality is examined. Additionally, the extent of the marginal external congestion cost are estimated from data for Central London. On a variety of streets and for ordinary congestion, the METC is in the region of 0.2 minutes per vkm. For periods of high ordinary congestion and high elasticity of speed with respect to density, the METC is likely to be much higher. The method proposed in this thesis for calculating the very short run (ie immediate) METC is identical to the conventional method. For periods of ordinary congestion with little variation in both speed from free flow and elasticity of speed with respect to density, the method proposed here gives very similar results to the conventional method. When speeds vary markedly across time and the speed elasticity move towards negative one, the two methods give markedly different results. In these circumstances, the new method gives very different estimates of the METCs and the elasticity of demand for transport with respect to journey time (representing the effect of deterred demand) becomes very important in determining the METC.

The new method gives estimates of the METC for periods of hypercongestion. The new method explains the generation of external effect in periods of hypercongestion. In particular, the external effect is reinforced through periods of hypercongestion as the elasticity of speed respect to density is equal to or exceeds negative one. The external effect can only diminish during periods of ordinary congestion. Thus, the METC is much higher at the beginning of a period of hypercongestion than at the end of the hypercongestion period. The empirical analysis of hypercongestion is continued in the next chapter.

The different estimated METCs for different habitual or random types of demand for road transport are briefly considered. They are shown to raise difficult issues for the implementation of a first best Pigovian taxing policy with regard to types of road user and identifying these types. More generally the signalling of the different external costs of road use and speeds of adjustment of deterred demands are seen to be important.

The estimated METCs are presented as indicative and have a large margin of potential numerical error. It is important to note that the estimates and theory considered in this Chapter take account of the congestion cost from longer duration of journeys but not of the costs of having to alter the timing of journeys.